ARTICLE

doi:10.1038/nature12586

Reprogramming *in vivo* produces teratomas and iPS cells with totipotency features

María Abad[1], Lluc Mosteiro[1], Cristina Pantoja[1], Marta Cañamero[2], Teresa Rayon[3], Inmaculada Ors[3], Osvaldo Graña[4], Diego Megías[5], Orlando Domínguez[6], Dolores Martínez[7], Miguel Manzanares[3], Sagrario Ortega[8] & Manuel Serrano[1]

Reprogramming of adult cells to generate induced pluripotent stem cells (iPS cells) has opened new therapeutic opportunities; however, little is known about the possibility of *in vivo* reprogramming within tissues. Here we show that transitory induction of the four factors *Oct4, Sox2, Klf4* and *c-Myc* in mice results in teratomas emerging from multiple organs, implying that full reprogramming can occur *in vivo*. Analyses of the stomach, intestine, pancreas and kidney reveal groups of dedifferentiated cells that express the pluripotency marker NANOG, indicative of *in situ* reprogramming. By bone marrow transplantation, we demonstrate that haematopoietic cells can also be reprogrammed *in vivo*. Notably, reprogrammable mice present circulating iPS cells in the blood and, at the transcriptome level, these *in vivo* generated iPS cells are closer to embryonic stem cells (ES cells) than standard *in vitro* generated iPS cells. Moreover, *in vivo* iPS cells efficiently contribute to the trophectoderm lineage, suggesting that they achieve a more plastic or primitive state than ES cells. Finally, intraperitoneal injection of *in vivo* iPS cells generates embryo-like structures that express embryonic and extraembryonic markers. We conclude that reprogramming *in vivo* is feasible and confers totipotency features absent in standard iPS or ES cells. These discoveries could be relevant for future applications of reprogramming in regenerative medicine.

Reprogramming into pluripotency remains an intense field of investigation that is providing many insights about cellular plasticity[1,2]. Cellular reprogramming has been achieved under carefully controlled *in vitro* culture conditions[3], whereas the *in vivo* tissue microenvironment is, in principle, conducive to cellular differentiation and opposed to reprogramming. However, we took note of remarkable examples in mice in which the normally irreversible state of cellular differentiation has been altered, inducing direct conversions *in vivo* from one cell type into a different one[4–10]. Encouraged by these precedents, we have attempted to achieve reprogramming *in vivo*.

Generation of reprogrammable mice

We have generated reprogrammable mice similar, but not identical, to others previously described[11–13]. A total of four transgenic mouse lines were obtained, each one carrying the transcriptional activator (rtTA) within the ubiquitously-expressed *Rosa26* locus[14] and a single copy of a lentiviral doxycycline-inducible polycistronic cassette encoding the four murine factors *Oct4* (also known as *Pou5f1*), *Sox2, Klf4* and *c-Myc*[15] (Fig. 1a; Extended Data Fig. 1a). In two of the four transgenic lines, the cassette was highly induced in most tissues (Extended Data Fig. 1b) and mouse embryonic fibroblasts (MEFs) from these lines were efficiently reprogrammed *in vitro* upon addition of doxycycline (Extended Data Fig. 1c, d). The other two transgenic lines did not express the cassette and their derived MEFs did not reprogram upon doxycycline addition. We have named the two functional transgenic lines as i4F-A and i4F-B, i4F standing for 'inducible four factors'. We determined the integration sites of the transgenes, which in the case of line i4F-A is within an intron of the *Neto2* gene, and in the case of line i4F-B is within an intron of the *Pparg* gene (Extended Data Fig. 2a). Transcription of these two genes remained unaltered in a number of tissues, either with or without doxycycline (Extended Data Fig. 2b). We conclude that transgenic lines i4F-A and i4F-B contain a functional inducible reprogramming transgene that is expressed in most tissues without affecting the resident endogenous genes.

Reprogrammable mice generate teratomas

To test the possibility of *in vivo* reprogramming, we first treated i4F-A and i4F-B mice continuously with a high dose of doxycycline (1 mg ml^{-1}) in the drinking water. This treatment resulted in weight loss and severe morbidity in both transgenic lines after 1 week. Histological examination of the mice revealed alterations in many tissues, particularly profound in the intestine and pancreas. The intestinal epithelium showed a generalized cytological and architectural dysplasia (Extended Data Fig. 3a), probably responsible for the weight loss. A similar phenotype has been reported for mice with transgenic expression of *Oct4* or *c-Myc*[14,16]. In the case of the pancreas, mice presented multifocal dysplasia (Extended Data Fig. 3b). Taking into account these observations, we tested two milder induction protocols that turned out to be compatible with the long-term survival of the mice. In particular, 2.5-week treatment with low doxycyline (0.2 mg ml^{-1}) or 1-week treatment with high doxycycline (1 mg ml^{-1}), both followed by doxycycline withdrawal. Remarkably, after a variable period of time, treated mice succumbed to the presence of tumoral masses (Fig. 1b; Extended Data Fig. 4a), most of which consisted of teratomas (Fig. 1c; Extended Data Fig. 4b). Teratomas are a particular class of tumours that originate from pluripotent cells after a process of expansion and disorganized differentiation. Most of the teratomas (32/45, 71%) were well differentiated and presented abundant examples of the three embryonic germ layers (Fig. 1d). Therefore, the presence of teratomas in our reprogrammable mice is indicative of reprogramming into full pluripotency. Mice treated with the long-induction/low-doxycycline protocol developed teratomas faster and at a higher incidence rate than those treated with the short-induction/

[1]Tumour Suppression Group, Spanish National Cancer Research Centre (CNIO), Madrid E-28029, Spain. [2]Histopathology Unit, Spanish National Cancer Research Centre (CNIO), Madrid E-28029, Spain. [3]Cardiovascular Development and Repair Department, Spanish National Cardiovascular Research Centre (CNIC), Madrid E-28029, Spain. [4]Bioinformatics Unit, Spanish National Cancer Research Centre (CNIO), Madrid E-28029, Spain. [5]Confocal Microscopy Unit, Spanish National Cancer Research Centre (CNIO), Madrid E-28029, Spain. [6]Genomics Unit, Spanish National Cancer Research Centre (CNIO), Madrid E-28029, Spain. [7]Flow Cytometry Unit, Spanish National Cancer Research Centre (CNIO), Madrid E-28029, Spain. [8]Transgenic Mice Unit, Spanish National Cancer Research Centre (CNIO), Madrid E-28029, Spain.

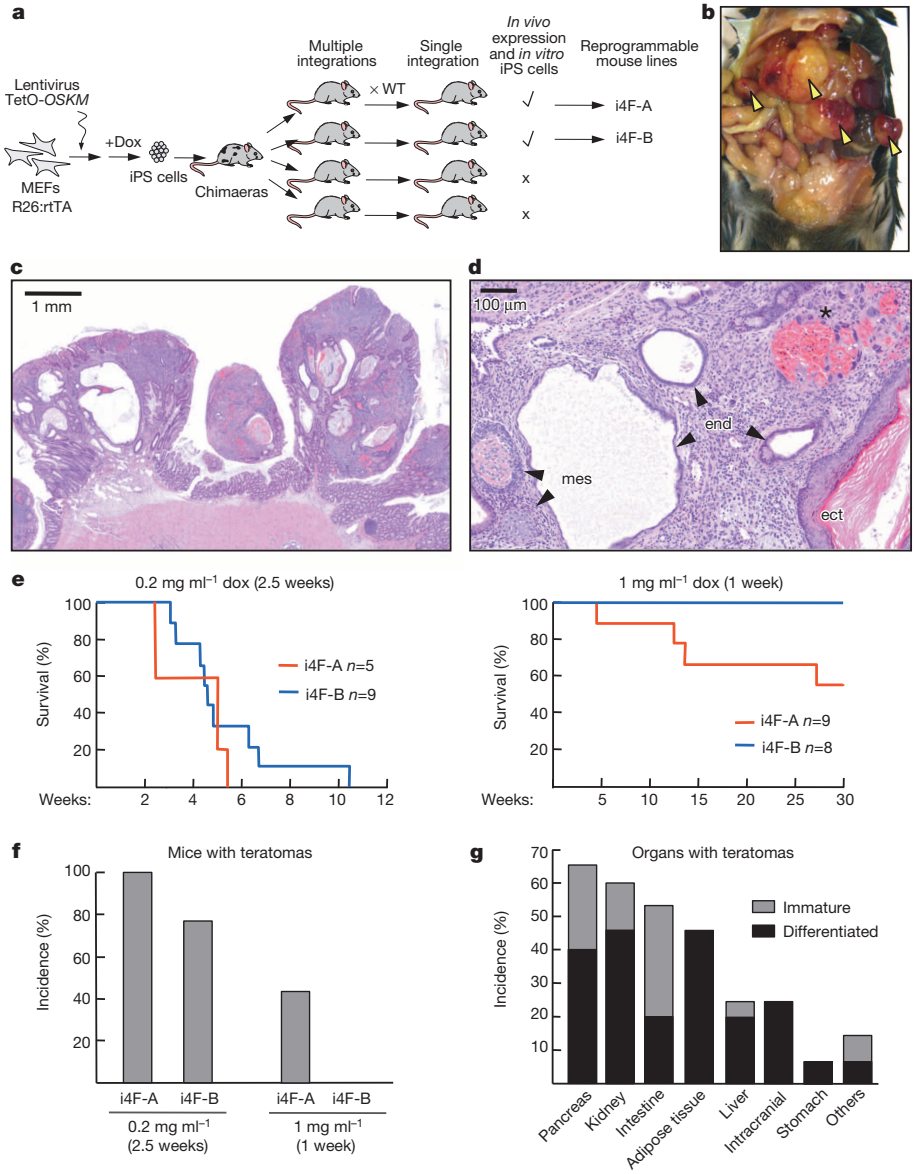

Figure 1 | Generation of teratomas upon *in vivo* induction of the four factors *Oct4*, *Sox2*, *Klf4* and *c-Myc*. **a**, Reprogrammable mouse generation. **b**, Reprogrammable mouse with multiple teratomas (arrowheads). **c**, Teratomas in the intestine of a reprogrammable mouse. **d**, Histological section of a teratoma with mesoderm (mes), endoderm (end) and ectoderm (ect). Asterisk indicates giant trophoblast cells and haemorrhages. **e**, Survival of reprogrammable mice after the indicated doxycycline treatments. Time refers to the initiation of the treatments. **f**, Incidence of teratomas. Data corresponds to their time of death or week 30. **g**, Localization of teratomas in mice with teratomas.

high-doxycycline protocol (Fig. 1e). The incidence of teratomas was higher in line i4F-A than in i4F-B (Fig. 1f), and in both lines and protocols, teratomas appeared in a variety of organs (Fig. 1g). Reprogrammable mice that were not treated with doxycycline remained healthy at least during 2 years of observation, indicating the absence of leaky expression of the reprogramming cassette. The presence of multiples teratomas in both lines implies that reprogramming into pluripotency is feasible within *in vivo* conditions.

In vivo reprogramming occurs in multiple tissues

Previous work has shown that haematopoietic progenitors can reprogram with high efficiency[17]. This, together with the broad distribution of haematopoietic cells within the organism, led us to consider that teratomas in our reprogrammable mice could originate from cells of the haematopoietic lineage. To address this, we performed bone marrow transplants into lethally irradiated hosts. In one setting, bone marrow (BM) from reprogrammable mice (i4F-BM) was transplanted into wild-type hosts and, in the reciprocal transplantation, wild-type bone marrow was transplanted into reprogrammable mice. Interestingly, both types of bone marrow reconstituted mice developed multiple teratomas upon induction (Fig. 2a, b). These results suggest that haematopoietic and non-haematopoietic cells can both be reprogrammed *in vivo*. Of note, the teratomas present in i4F-BM transplanted mice were not emerging from organs, but outgrew attached to the serous membranes of the thoracic and abdominal cavities, whereas reprogrammable mice (either whole-body or transplanted with wild-type bone marrow) presented teratomas within multiple organs, as previously mentioned (Fig. 1g).

The above results prompted us to look for early reprogramming events in non-haematopoietic cells. In particular, we focused on the stomach, intestine, pancreas and kidney of whole-body reprogrammable mice. We performed double immunohistochemistry against the epithelial marker cytokeratin 19 (CK19, also known as KRT19) and the pluripotency marker NANOG. We found aberrant individual gastric glands and intestinal crypts (in the small and large intestine) that had lost or decreased CK19 and expressed NANOG (Fig. 2c, d). In some cases the entire gland or crypt was aberrant, whereas in others intermediate situations were found. In the pancreas, we observed both acinar-like (CK19-negative) and ductal-like (CK19-positive) structures with NANOG-positive cells (Fig. 2e). In the kidney, which does not undergo major detectable morphological changes upon doxycycline induction but has a high incidence of teratomas (Fig. 1g), we found isolated kidney tubules expressing NANOG (Extended Data Fig. 4c). In general, the number of reprogramming events evidenced

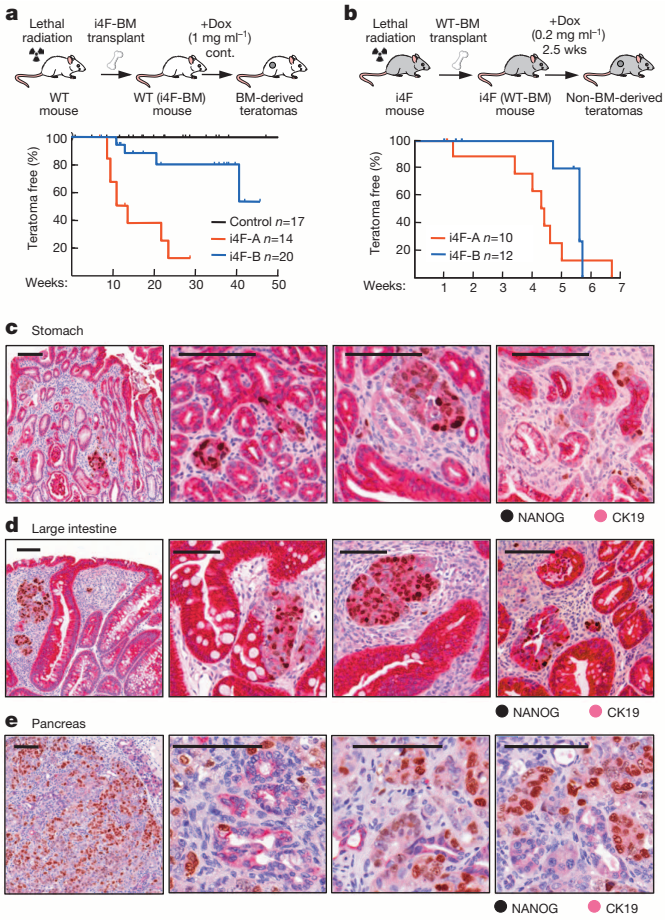

Figure 2 | Many cell types are reprogrammed *in vivo*. **a**, Incidence of teratomas in wild-type mice transplanted with reprogrammable bone marrow (BM). Time refers to the initiation of the treatment. **b**, Same as **a** in reprogrammable mice transplanted with wild-type BM. Ticks indicate censored mice dead without teratomas due to pulmonary oedemas secondary to irradiation (**a**) or systemic i4F induction (**b**). **c**, Double immunohistochemistry of NANOG (dark brown) and cytokeratin 19 (CK19, magenta) in the stomach of whole-body reprogrammable mice. **d**, Same staining as **c** in the large intestine. **e**, Same staining as **c** in the pancreas. All scale bars correspond to 100 μm.

by NANOG (Fig. 2d) was clearly lower than the number of cells expressing the reprogramming cassette (Extended Data Fig. 3a), implying that reprogramming *in vivo* is a low efficiency process that likely involves stochastic events, similar to what happens during *in vitro* reprogramming[18,19]. The presence of isolated NANOG-positive structures, such as intestinal crypts or kidney tubules, probably reflects the clonal expansion of an individual reprogramming event. These observations support the concept that reprogramming occurs *in situ*, at least in the case of the epithelial cells of the stomach, intestine, pancreas and kidney.

Reprogrammable mice present iPS cells in the blood

Given the feasibility of *in vivo* reprogramming, we wondered whether it was possible to detect circulating iPS cells in the bloodstream. To address this, the cellular fraction of the blood from induced reprogrammable mice ($\sim 10^6$ leukocytes) was seeded into plates with feeder fibroblasts and iPS cell culture medium (all procedures after blood extraction were performed in the absence of doxycycline). Remarkably, after a variable period of time (1–2 weeks), colonies with iPS cell morphology were visible (Fig. 3a). These colonies were expanded (Fig. 3b) and were found to express pluripotency markers (Fig. 3c, d; Extended Data Fig. 5a) and to have silenced the lentiviral reprogramming cassette (Extended Data Fig. 5b). Moreover, *in vivo* iPS cells generated subcutaneous teratomas with representation of the three germ layers (Fig. 3e), produced mouse chimaeras (Fig. 3f) and contributed to the germ lineage (Extended Data Fig. 5c). Therefore, we conclude that bona fide iPS cells can be isolated from the blood of reprogrammable mice. Of note, colonies of iPS cells were obtained from whole-body reprogrammable mice, as well as from wild-type mice with reprogrammable bone marrow and from reprogrammable mice with wild-type bone marrow (Extended Data Fig. 5d). Therefore, both haematopoietic and non-haematopoietic cells can generate *in vivo* circulating iPS cells. The overall frequency of mice with colony-forming iPS cells was 6.5% (5/77) (Fig. 3g), and this frequency was similar in the two transgenic lines (Extended Data Fig. 5d). In those blood samples that were positive for iPS cells colony formation, the number of colonies obtained was variable (9 ± 5) (Extended Data Fig. 5d). We will refer to the circulating iPS cells as *in vivo* iPS cells to distinguish them from the standard *in vitro* generated ones.

Transcriptomic analysis of *in vivo* iPS cells

To further characterize the *in vivo* iPS cells, we performed messenger RNA deep sequencing. We sequenced *in vivo* iPS cells ($n = 6$ independent clones), *in vitro* iPS cells ($n = 5$ independent clones derived from i4F-MEFs) and ES cells (JM8.F6 (ref. 20), Bruce4 (ref. 21) and CNIO in-house made C57BL6.10). The homogeneity of the samples of each cell type was confirmed by the high intra-group correlation coefficients (Extended Data Fig. 6a). Furthermore, all of the 14 transcriptomes analysed were highly similar regardless of their origin (the lowest pairwise correlation coefficient was $r = 0.93$) (Extended Data Fig. 6a). Interestingly, inter-group comparisons by scatter plots, volcano plots and Pearson coefficient correlations indicated a higher degree of similarity between *in vivo* iPS and ES cells ($r = 0.997$), than between the other two possible combinations (*in vivo* iPS cells vs *in vitro* iPS cells, $r = 0.971$; ES cells vs *in vitro* iPS cells, $r = 0.966$) (Extended Data Fig. 6c). Moreover, unsupervised hierarchical clustering of the 14 transcriptomes classified together *in vivo* iPS cells and ES cells, and separated them from *in vitro* iPS cells (Fig. 3h). The same classification was obtained using principal component analysis, which is another unbiased method to quantify the degree of similarity between large data sets (Extended Data Fig. 6b). The lists of differentially expressed genes were obtained for further analyses (Supplementary Tables 1–3). Interestingly, among the genes commonly upregulated in *in vivo* iPS and ES cells compared to *in vitro* iPS cells (a total of 51 genes; Supplementary Table 4) there were several pluripotency genes, including *Gbx2*, *Lin28a*, *Utf1* and others associated with pluripotency, such as *Epcam* and *Ccne1*. The upregulation of these genes in *in vivo* iPS and ES cells was validated by quantitative PCR with reverse transcription (qRT–PCR) (Extended Data Fig. 7a). Having established that *in vivo* iPS cells are extremely similar to ES cells, we focused on those few genes that were differentially expressed in *in vivo* iPS cells relative to ES cells and *in vitro* iPS cells (Fig. 3i; Supplementary Table 5). Among these genes, we validated the upregulation of *Nlrp4f* (known to be enriched at the morula state)[22], *Etv4* (a transcription factor of the *Ets* family expressed during early development)[23], *Ppm1j* (a protein phosphatase transcriptionally upregulated upon GSK3β inhibition)[24], *8430410A17Rik* (a gene consistently found associated with stemness)[25] and *Tgm1* (Fig. 3j; Extended Data Fig. 7b), and the downregulation of *Mmp12* and *Tnc* (both encoding components or regulators of the extracellular matrix) (Fig. 3j). Importantly, the pattern of expression of these genes was similar in *in vivo* iPS cells and in morulas (Fig. 3j; Extended Data Fig. 7b), thus suggesting that *in vivo* iPS cells and morulas share transcriptional features that are absent in ES cells or in *in vitro* iPS cells. We conclude that *in vivo* iPS cells are extremely similar to ES cells, but present differentially expressed genes that could conceivably confer additional properties to the *in vivo* iPS cells.

In vivo iPS cells contribute to the trophectoderm

We noted that the teratomas that appeared in reprogrammable mice often presented areas with large cells that resemble trophoblast giant

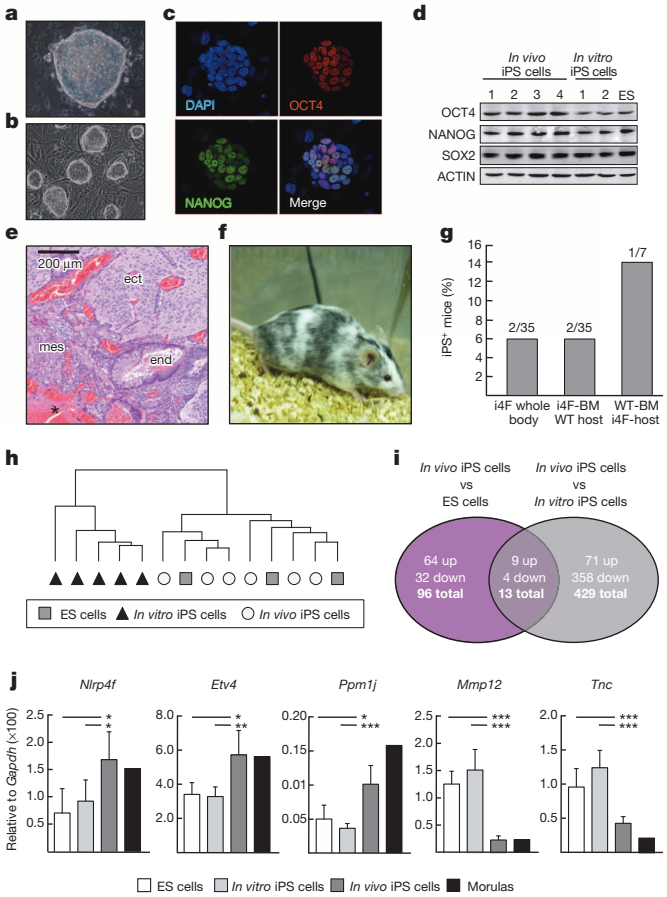

Figure 3 | Isolation and characterization of *in vivo* iPS cells. **a**, *In vivo* iPS cell colony 10 days after blood plating. **b**, Expansion of *in vivo* iPS cells. **c**, Immunofluorescence of *in vivo* iPS cell colony. **d**, Immunoblot of *in vivo* iPS cells, *in vitro* iPS cells (no. 1 from i4F MEFs; no. 2 from MEFs infected with lenti-OSKM) and C57BL/6.10 ES cells. **e**, Subcutaneous teratoma from *in vivo* iPS cells injection. Asterisk indicates giant trophoblast cells and haemorrhages. **f**, *In vivo* iPS cells derived chimaera. **g**, Frequency of *in vivo* iPS cells isolation. **h**, Unsupervised hierarchical clustering of *in vivo* iPS cells, *in vitro* iPS cells and ES cells (6, 5 and 3 clones respectively). **i**, Venn diagram of differentially expressed genes. **j**, qPCR analysis of differentially expressed genes in the same clones as in **h**. Average ± s.d. and unpaired two-tailed Student's *t*-test are shown. $*P < 0.05$; $**P < 0.01$; $***P < 0.001$.

cells associated with internal haemorrhages, altogether characteristic of placental tissue (Fig. 4a; see also examples in Figs 1d and 3e). Indeed, this was confirmed by the expression of PL-1 (placental lactogen 1 or chorionic somatomammotropin hormone 1) and CK8 (cytokeratin 8 or KRT8), which are both markers of trophoblast giant cells (Fig. 4a). We were intrigued by this observation because trophoblast differentiation is rare in teratomas produced by ES cells[26]. To further explore this, we subjected ES cells, *in vitro* iPS cells and *in vivo* iPS cells to culture conditions that favour differentiation into trophoblast stem cells (namely, removal of LIF and addition of FGF4 and heparin)[26–28]. After 5 days, *in vivo* iPS cells formed abundant colonies with a flattened morphology characteristic of trophoblast stem cells. In contrast, *in vitro* iPS and ES cells produced a lower number of colonies and only few of them showed trophoblast stem cell like morphology (Fig. 4b). Furthermore, *in vivo* iPS cells upregulated markers of trophectoderm lineage (*Cdx2*, *Fgfr2* and *Eomes*) to a larger extent than equally treated *in vitro* iPS or ES cells (Fig. 4c; Extended Data Fig. 8a). The upregulation of *Cdx2* in *in vivo* iPS cells was confirmed by immunofluorescence (Fig. 4d). As a control, markers of ectoderm (*Sox1*), mesoderm (*T*) and endoderm (*Gata6*) lineages showed similar levels of expression among all the cell types examined (Extended Data Fig. 8a). Moreover, upon removal of FGF4 and heparin, trophoblast stem cell differentiated *in vivo* iPS cells generated trophoblast giant cells (Fig. 4e).

Based on the above observations, we tested the capacity of *in vivo* iPS cells to contribute to the trophectoderm. For this, GFP-expressing *in vivo* iPS and ES cells were aggregated or microinjected into morulas (either wild type or carrying a Katushka red fluorescent transgene[29]) and the resulting blastocysts were examined. As expected, both cell types, *in vivo* iPS and ES cells, efficiently contributed (100%) to the inner cell mass (ICM). Interestingly, *in vivo* iPS cells also contributed to the polar trophectoderm (surrounding the ICM) and to the mural trophectoderm (Fig. 4f; Extended Data Fig. 8b). Altogether, *in vivo* iPS cells contributed to the trophectoderm with a remarkable efficiency (56%), which was in contrast to ES cells (0%) (Fig. 4g)[30]. To test whether the *in vivo* iPS cells actually contribute to the formation of the placenta, we examined chimaeric E14.5 embryos generated with GFP-expressing *in vivo* iPS cells and we observed a high degree of chimaerism both in the embryo proper as well as in the placenta (Fig. 4h, i; Extended Data Fig. 8c). Previous investigators have reported that ES cells and standard iPS cells can transitorily access a totipotency-like state similar to the 2-cell blastomeres (2C state)[31]. We wondered whether *in vivo* iPS cells are enriched in the 2C state, however, we could not see upregulation of the 2C markers *Zscan4*, *MuERV-L* and *IAP* (Extended Data Fig. 9). Therefore, *in vivo* iPS cells do not seem to be enriched in the 2C state, although, as shown above (Fig. 3j), they share transcriptional features with morulas. Together, we conclude that *in vivo* reprogramming confers a pluripotency state that, in contrast to ES cells or standard *in vitro* iPS cells, can readily access the trophectodermal lineage.

In vivo iPS cells generate embryo-like structures

During the course of the above analyses we observed the presence of small cysts in the thoracic and abdominal cavities of two reprogrammable mice (from a total of 77 induced reprogrammable mice) (Fig. 5a). These cysts were often detached from the surrounding organs and from the lining of the abdominal and thoracic cavities (Fig. 5a). The cysts were formed by membranous structures and, based on their detailed characterization (see below), we refer to them as embryo-like structures. We wondered whether *in vivo* iPS cells could also form embryo-like structures when injected intraperitoneally into wild-type mice. Remarkably, in addition to the expected teratomas, a fraction of mice injected with *in vivo* iPS cells contained embryo-like structures, in contrast to the mice injected with *in vitro* iPS or ES cells (Fig. 5b). Immunohistological analyses of the embryo-like structures indicated the presence of cell layers and cellular areas expressing lineage markers SOX2 (ectoderm), T/BRACHYURY (mesoderm), or GATA4 (endoderm) (Fig. 5c; Extended Data Fig. 10). In addition, these embryo-like structures also expressed CDX2 (Fig. 5c; Extended Data Fig. 10), indicative of trophectoderm lineage[32], and presented cell layers with the typical border morphology of the yolk sac endoderm which co-expressed α-fetoprotein (AFP) and cytokeratin 8 (CK8) (Fig. 5c; Extended Data Fig. 10), both characteristic of the visceral endoderm of the yolk sac[33]. Finally, embryo-like structures presented regions resembling blood islands, internally lined by the endothelial cell surface marker LYVE-1 (ref. 34) and with associated nucleated erythrocytes positive for the TER-119 marker (Fig. 5d), highly suggestive of yolk sac associated erythropoiesis. We conclude that *in vivo* iPS cells possess an unprecedented cell-autonomous capacity to produce embryo-like structures containing the three embryonic germ layers together with structures reminiscent of the extraembryonic ectoderm and the yolk sac. This reinforces the concept that *in vivo* reprogramming allows the acquisition of totipotency features that are absent in ES cells or in standard *in vitro* reprogrammed iPS cells.

Conclusion

In this work, we demonstrate that the four factors *Oct4*, *Sox2*, *Klf4* and *c-Myc* can induce dedifferentiation and pluripotency in a variety of cell types *in vivo*, including cells from the haematopoietic lineage, as

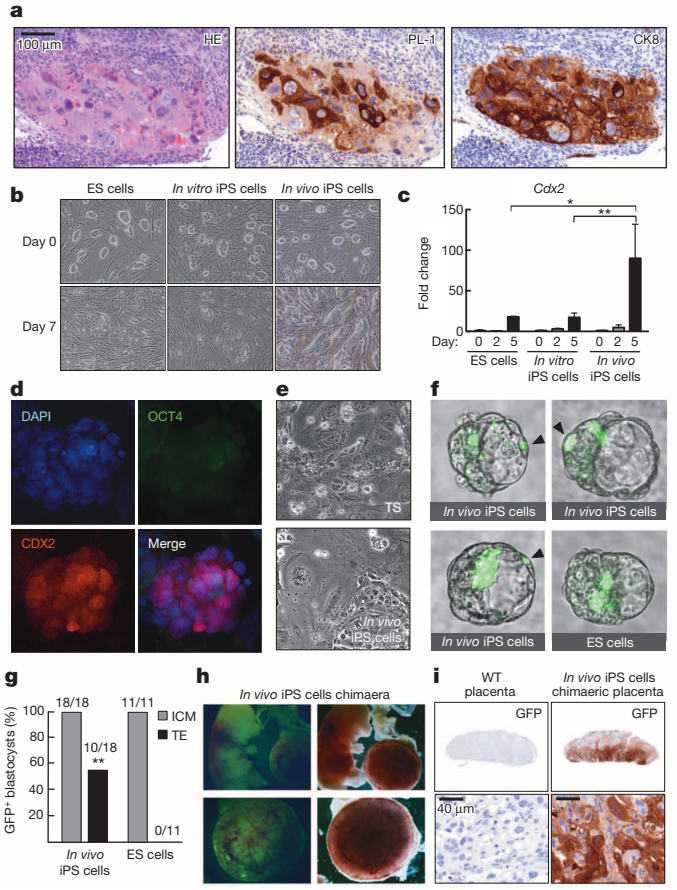

Figure 4 | *In vivo* iPS cells efficiently contribute to the trophectoderm. **a**, Teratomas with trophoblast giant cells. **b**, Trophoblast stem cell differentiation of the indicated cells. **c**, *Cdx2* expression in *in vivo* iPS cells, *in vitro* iPS cells and ES cells (6, 5 and 3 clones, respectively) during TS differentiation, relative to day 0. Average ± s.d. and unpaired, two-tailed Student's *t*-test are shown: $*P < 0.05$, $**P < 0.01$. **d**, Immunofluorescence of *in vivo* iPS cells derived trophoblast stem cells. **e**, Giant cells differentiated from trophoblast stem cells and *in vivo* iPS cells derived trophoblast stem cells. **f**, Chimaeric blastocysts from GFP *in vivo* iPS cells and GFP-ES cells. Arrowheads mark GFP^+ trophectoderm cells. **g**, Frequency of blastocysts with GFP^+ trophectoderm cells from *in vivo* iPS cells ($n = 2$ clones) and ES cells (JM8.F6). Fisher's exact test: $**P < 0.01$. **h**, GFP *in vivo* iPS cells chimaeric embryo and placenta. **i**, Immunostaining against GFP.

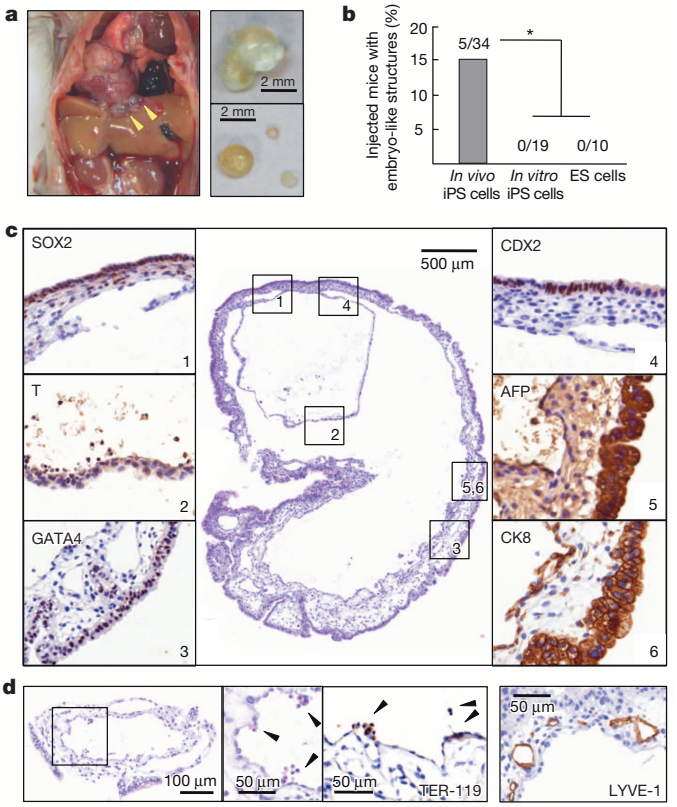

Figure 5 | *In vivo* reprogramming and *in vivo* iPS cells generate embryo-like structures. **a**, Cysts in the abdominal cavity of a reprogrammable mouse. **b**, Frequency of embryo-like structures after intraperitoneal injection of *in vivo* iPS cells (3 clones), *in vitro* iPS cells (2 clones) and ES cells (JM8.F6). Fisher's exact test: $*P < 0.05$. **c**, Cyst generated by intraperitoneal injection. Left panels, germ layer markers: SOX2 (ectoderm), T/BRACHYURY (mesoderm) and GATA4 (endoderm). Right panels, extraembryonic markers: CDX2 (trophectoderm), and AFP and CK8, both specific for visceral endoderm of the yolk sac. **d**, Cyst generated by intraperitoneal injection presenting TER-119$^+$ nucleated erythrocytes and LYVE-1$^+$ endothelial cells in structures resembling yolk sac blood islands.

well as epithelial cells from the stomach, intestine, pancreas and kidney. In the context of previous examples of *in vivo* cellular conversions[4–10], our results notably extend the concept of *in vivo* plasticity to many tissues and to the extreme case of generating embryonic pluripotent cells, a cell type that is absent in the adult organism. Previous investigators have shown that intentionally incomplete *in vitro* reprogramming with the four factors triggers a dedifferentiated cellular state that can have advantageous differentiation properties[35,36]. In this regard, partial or transient activation of the four factors *in vivo* is an attractive approach for regenerative purposes.

Another important aspect of our work is the recovery of circulating iPS cells from the blood of induced reprogrammable mice, which can derive from both haematopoietic and non-haematopoietic cells. Notably, *in vivo* iPS and ES cells are extremely similar, and clearly separated from *in vitro* iPS cells. Despite the high similarity between *in vivo* iPS and ES cells, it is possible to detect differentially expressed genes among the two cell types. These differences may originate from differential epigenetic marks and/or self-sustained transcriptional networks, both of which are prominent regulators of pluripotency[37,38]. *In vivo* iPS cells present a remarkable capacity to undergo trophectoderm lineage differentiation, a property that is largely absent in ES cells (or *in vitro* iPS cells) under normal culture conditions. Finally, *in vivo* iPS cells have an unprecedented capacity to form embryo-like structures, including the three germ layers of the proper embryo and extraembryonic tissues, such as extraembryonic ectoderm and yolk sac like tissue with associated embryonic erythropoiesis. Together, we conclude that *in vivo* iPS cells represent a more primitive or plastic state than ES cells. Future work will explore the full capabilities of *in vivo* iPS cells.

METHODS SUMMARY

***In vivo* iPS cell isolation.** Peripheral blood (0.3–0.5 ml) was collected directly from the heart of doxycycline-induced i4F mice at the time of necropsy. After blood extraction, all procedures were performed in the absence of doxycycline. The recovered cells were plated on feeders and cultured in iPS cell medium.

Generation of embryo-like structures. Wild-type C57BL/6 mice were injected with 5×10^5 cells in 100 µl of iPS cell medium. When teratomas were palpable, usually around 2 months post-injection, mice were euthanized.

Online Content Any additional Methods, Extended Data display items and Source Data are available in the online version of the paper; references unique to these sections appear only in the online paper.

Received 4 March; accepted 23 August 2013.

Published online 11 September; corrected online 16 October 2013 (see full-text HTML version for details).

1. Takahashi, K. & Yamanaka, S. Induction of pluripotent stem cells from mouse embryonic and adult fibroblast cultures by defined factors. *Cell* **126,** 663–676 (2006).

2. Robinton, D. A. & Daley, G. Q. The promise of induced pluripotent stem cells in research and therapy. *Nature* **481,** 295–305 (2012).
3. Maherali, N. & Hochedlinger, K. Guidelines and techniques for the generation of induced pluripotent stem cells. *Cell Stem Cell* **3,** 595–605 (2008).
4. Cobaleda, C., Jochum, W. & Busslinger, M. Conversion of mature B cells into T cells by dedifferentiation to uncommitted progenitors. *Nature* **449,** 473–477 (2007).
5. Zhou, Q., Brown, J., Kanarek, A., Rajagopal, J. & Melton, D. A. *In vivo* reprogramming of adult pancreatic exocrine cells to β-cells. *Nature* **455,** 627–632 (2008).
6. Qian, L. *et al. In vivo* reprogramming of murine cardiac fibroblasts into induced cardiomyocytes. *Nature* **485,** 593–598 (2012).
7. Song, K. *et al.* Heart repair by reprogramming non-myocytes with cardiac transcription factors. *Nature* **485,** 599–604 (2012).
8. Banga, A., Akinci, E., Greder, L. V., Dutton, J. R. & Slack, J. M. *In vivo* reprogramming of $Sox9^+$ cells in the liver to insulin-secreting ducts. *Proc. Natl Acad. Sci. USA* **109,** 15336–15341 (2012).
9. Rouaux, C. & Arlotta, P. Direct lineage reprogramming of post-mitotic callosal neurons into corticofugal neurons *in vivo. Nature Cell Biol.* **15,** 214–221 (2013).
10. Torper, O. *et al.* Generation of induced neurons via direct conversion *in vivo. Proc. Natl Acad. Sci. USA* **110,** 7038–7043 (2013).
11. Stadtfeld, M., Maherali, N., Borkent, M. & Hochedlinger, K. A reprogrammable mouse strain from gene-targeted embryonic stem cells. *Nature Methods* **7,** 53–55 (2010).
12. Carey, B. W., Markoulaki, S., Beard, C., Hanna, J. & Jaenisch, R. Single-gene transgenic mouse strains for reprogramming adult somatic cells. *Nature Methods* **7,** 56–59 (2010).
13. Haenebalcke, L. *et al.* The ROSA26-iPSC mouse: a conditional, inducible, and exchangeable resource for studying cellular (de)differentiation. *Cell Rep.* **3,** 335–341 (2013).
14. Hochedlinger, K., Yamada, Y., Beard, C. & Jaenisch, R. Ectopic expression of Oct-4 blocks progenitor-cell differentiation and causes dysplasia in epithelial tissues. *Cell* **121,** 465–477 (2005).
15. Carey, B. W. *et al.* Reprogramming of murine and human somatic cells using a single polycistronic vector. *Proc. Natl Acad. Sci. USA* **106,** 157–162 (2009).
16. Finch, A. J., Soucek, L., Junttila, M. R., Swigart, L. B. & Evan, G. I. Acute overexpression of Myc in intestinal epithelium recapitulates some but not all the changes elicited by Wnt/beta-catenin pathway activation. *Mol. Cell. Biol.* **29,** 5306–5315 (2009).
17. Eminli, S. *et al.* Differentiation stage determines potential of hematopoietic cells for reprogramming into induced pluripotent stem cells. *Nature Genet.* **41,** 968–976 (2009).
18. Yamanaka, S. Elite and stochastic models for induced pluripotent stem cell generation. *Nature* **460,** 49–52 (2009).
19. Hanna, J. *et al.* Human embryonic stem cells with biological and epigenetic characteristics similar to those of mouse ESCs. *Proc. Natl Acad. Sci. USA* **107,** 9222–9227 (2010).
20. Pettitt, S. J. *et al.* Agouti C57BL/6N embryonic stem cells for mouse genetic resources. *Nature Methods* **6,** 493–495 (2009).
21. Hughes, E. D. *et al.* Genetic variation in C57BL/6 ES cell lines and genetic instability in the Bruce4 C57BL/6 ES cell line. *Mamm. Genome* **18,** 549–558 (2007).
22. Assou, S. *et al.* Transcriptome analysis during human trophectoderm specification suggests new roles of metabolic and epigenetic genes. *PLoS ONE* **7,** e39306 (2012).
23. Koo, T. B. *et al.* Differential expression of the PEA3 subfamily of ETS transcription factors in the mouse ovary and peri-implantation uterus. *Reproduction* **129,** 651–657 (2005).
24. Yao, X. Q. *et al.* Glycogen synthase kinase-3β regulates leucine-309 demethylation of protein phosphatase-2A via PPMT1 and PME-1. *FEBS Lett.* **586,** 2522–2528 (2012).
25. Glover, C. H. *et al.* Meta-analysis of differentiating mouse embryonic stem cell gene expression kinetics reveals early change of a small gene set. *PLOS Comput. Biol.* **2,** e158 (2006).
26. Koh, K. P. *et al.* Tet1 and Tet2 regulate 5-hydroxymethylcytosine production and cell lineage specification in mouse embryonic stem cells. *Cell Stem Cell* **8,** 200–213 (2011).
27. Lu, C. W. *et al.* Ras-MAPK signaling promotes trophectoderm formation from embryonic stem cells and mouse embryos. *Nature Genet.* **40,** 921–926 (2008).
28. Ng, R. K. *et al.* Epigenetic restriction of embryonic cell lineage fate by methylation of Elf5. *Nature Cell Biol.* **10,** 1280–1290 (2008).
29. Diéguez-Hurtado, R. *et al.* A Cre-reporter transgenic mouse expressing the far-red fluorescent protein Katushka. *Genesis* **49,** 36–45 (2011).
30. Beddington, R. S. & Robertson, E. J. An assessment of the developmental potential of embryonic stem cells in the midgestation mouse embryo. *Development* **105,** 733–737 (1989).
31. Macfarlan, T. S. *et al.* Embryonic stem cell potency fluctuates with endogenous retrovirus activity. *Nature* **487,** 57–63 (2012).
32. Pfister, S., Steiner, K. A. & Tam, P. P. Gene expression pattern and progression of embryogenesis in the immediate post-implantation period of mouse development. *Gene Expr. Patterns* **7,** 558–573 (2007).
33. Conley, B. J., Trounson, A. O. & Mollard, R. Human embryonic stem cells form embryoid bodies containing visceral endoderm-like derivatives. *Fetal Diagn. Ther.* **19,** 218–223 (2004).
34. Gordon, E. J., Gale, N. W. & Harvey, N. L. Expression of the hyaluronan receptor LYVE-1 is not restricted to the lymphatic vasculature; LYVE-1 is also expressed on embryonic blood vessels. *Dev. Dyn.* **237,** 1901–1909 (2008).
35. Thier, M. *et al.* Direct conversion of fibroblasts into stably expandable neural stem cells. *Cell Stem Cell* **10,** 473–479 (2012).
36. Kurian, L. *et al.* Conversion of human fibroblasts to angioblast-like progenitor cells. *Nature Methods* **10,** 77–83 (2013).
37. Halley, J. D. *et al.* Self-organizing circuitry and emergent computation in mouse embryonic stem cells. *Stem Cell Res.* **8,** 324–333 (2012).
38. Marks, H. *et al.* The transcriptional and epigenomic foundations of ground state pluripotency. *Cell* **149,** 590–604 (2012).

Supplementary Information is available in the online version of the paper.

Acknowledgements We are grateful to M.Torres for advice, and to K. Hochedlinger and R. Jaenisch for reagents. We also thank F. Beier, R. Serrano and N. Soberón for technical support. Work in the laboratory of M.S. is funded by the CNIO and by grants from the Spanish Ministry of Economy (MINECO, SAF), the Regional Government of Madrid (ReCaRe), the European Union (RISK-IR), the European Research Council (ERC Advanced Grant), the Botin Foundation, the Ramon Areces Foundation and the AXA Foundation. Work in the laboratory of M.M. is funded by grants from the MINECO (BFU), the Regional Government of Madrid (Cell-DD) and the ProCNIC Foundation. The funders had no role in study design, data collection and analysis, decision to publish, or preparation of the manuscript.

Author Contributions M.A. performed most of the experiments, contributed to experimental design, data analysis, discussion and writing; L.M. performed a substantial amount of experimental work, contributed to experimental design, data analysis, discussion and writing; C.P. contributed to experimental work, data analysis, discussion and writing; M.C. performed all the histopathological and immunohistochemical analyses; T.R. and I.O. contributed to the trophoblast stem cell and giant cell differentiation assays; O.G. analysed the RNAseq data; D. Megías supervised and helped with the confocal microscopy; O.D. performed RNAseq and determined the lentiviral genomic insertion sites; D. Martínez performed cell sorting and contributed to the bone marrow and peripheral blood analyses; M.M. supervised trophoblast differentiation assays and gave advice; S.O. generated the transgenic mice, constructed chimeras, and perfomed morula and blastocyst assays; M.S. designed and supervised the study, secured funding, analysed the data, and wrote the manuscript. All authors discussed the results and commented on the manuscript.

Author Information The primary RNA-seq data has been deposited in the GEO repository under accession number GSE48364. Reprints and permissions information is available at www.nature.com/reprints. The authors declare no competing financial interests. Readers are welcome to comment on the online version of the paper. Correspondence and requests for materials should be addressed to M.S. (mserrano@cnio.es).

METHODS

Generation of i4F reprogrammable mice. To generate reprogrammable mice, we transduced C57BL/6 mouse embryonic fibroblasts (MEFs) carrying a doxycycline-inducible transcriptional activator (rtTA) within the *Rosa26* locus[14] (generously provided by K. Hochedlinger) with a lentivirus carrying a doxycycline-inducible tetracistronic cassette with the four murine reprogramming factors (*Oct4, Sox2, Klf4, c-Myc*)[15] (Tet-O-FUW-OSKM, obtained from Addgene #20321). After lentiviral transduction, MEFs were treated with 1 μg ml^{-1} of doxycycline and colonies of iPS cells appeared after 1 week. Several iPS cells colonies were picked, expanded and microinjected into albino C57BL/6J-*Tyr*$^{c\text{-}2J}$/J E3.5 blastocysts (5–7 iPS cells per blastocyst) to obtain chimaeras. Chimaeric mice were backcrossed with C57BL6/J mice until the lentiviral transgenes were transmitted at Mendelian proportions (indicative of single integration site). The resulting reprogrammable i4F mice used in this study are in a pure C57BL6/J genetic background.

Southern blotting. Genomic DNA (tail tip) was digested overnight with BamHI and hybridized with probes designed to recognize exonic sequences of *Sox2* and *Klf4*. The probes were generated by PCR of genomic DNA with the following primers: *Sox2*-F: 5′-TACAGCATGATGCAGGAGCA-3′; *Sox2*-R: 5′-CTGGG CCATGTGCAGTCTAC-3′; *Klf4*-F: 5′-CAGCTTCAGCTATCCGATCC-3′; *Klf4*-R: 5′-CGCCTCTTGCTTAATCTTGG-3′.

Transgene insertion site determination. We performed gene walking as described[39]. Insertion sites were confirmed by PCR using primers against genomic sequences around the insertion site (*Neto2* in the case of line i4F-A, primer 5′-GCGTCA GGCAATTTATACTCTGG-3′; and *Pparg* in the case of line i4F-B, primer 5′-CA GCATCAAATGGCTCGGTA-3′) and against the lentiviral transgene (5′-GCAC CATCCAAAGGTCAGTG-3′).

Animal procedures. Animal experimentation at the CNIO, Madrid, was performed according to protocols approved by the CNIO-ISCIII Ethics Committee for Research and Animal Welfare (CEIyBA). Doxycycline (Sigma) was administered in the drinking water supplemented with 7.5% of sucrose. Experiments were performed indistinguishably with mice of both sexes and from 2 to 6 months of age. For bone marrow (BM) transplant, groups of 8 wild-type mice (C57BL6/J, 8–10-weeks old) per donor mouse were irradiated with 12 Gy. The following day, the bone marrow of the donor mice was harvested from the femora and tibiae and 2×10^6 – 2.5×10^6 cells, suspended in Leibovitz medium (Sigma, L5520), were intravenously injected per recipient. Experiments on transplanted mice were performed after a latency of at least 30 days to ensure BM reconstitution. For the intraperitoneal injections, wild-type mice were injected with 5×10^5 cells suspended in 100 μl of iPS cell medium. For subcutaneous teratomas, iPS or ES cells were trypsinized and 2×10^6 cells were subcutaneously injected into the flanks of immunocompromised nude mice (Swiss nude from Charles River). Teratomas were isolated when the diameter reached >1.5 cm and processed for histological analysis.

Cell culture. Primary mouse embryonic fibroblasts (MEFs) were obtained from embryos at E13.5 and cultured in DMEM supplemented with 10% of FBS and penicillin-streptomycin. The following C57BL6 ES cell lines were used: JM8.F6 (ref. 20), Bruce4 (ref. 21), and CNIO in-house made C57BL6.10. Cultures were routinely tested for mycoplasma and were always negative. ES and iPS cells were cultured over mitomycin-C inactivated feeder cells on gelatin-coated plates and in 'iPS medium': high-glucose DMEM supplemented with KSR (15%, Invitrogen), LIF (1,000 U ml^{-1}), non-essential amino acids, penicillin-streptomycin, glutamax and β-mercaptoethanol. For lentiviral transduction, we transfected HEK293T (5×10^6) cells with Tet-O-FUW-OSKM (Addgene #20321) and packaging vectors using Fugene HD (Roche). Viral supernatants were collected twice a day on two consecutive days starting 24 h after transfection and were used to infect ROSA26-rtTA MEFs, previously plated at a density of 2×10^5 cells per well in 6-well plates. Previous to infection, polybrene was added to the viral supernatants at a concentration of 8 μg ml^{-1}. For *in vitro* i4F reprogramming, i4F MEFs were plated at a density of 5×10^5 cells per well in 6-well gelatin-coated plates, and at a density of 3×10^5 for the kinetics assay. Infected MEFs or i4F-MEFs were cultured in iPS cell medium with doxycycline (1 μg ml^{-1}). Medium was changed every 48 h until iPS cell colonies appeared (after ~7 days of treatment). Reprogramming plates were stained for alkaline phosphatase activity (AP detection kit, Sigma-Aldrich). When indicated, ES cells or *in vivo* iPS cells were retrovirally infected with a vector expressing GFP (pMSCV-PIG) and infected cells were sorted by FACS.

***In vivo* iPS cell isolation.** Peripheral blood (0.3–0.5 ml) was collected directly from the heart of i4F mice at the time of necropsy, and was subjected to two rounds of erythrocyte lysis in ammonium chloride solution (Stem Cells). First round of lysis with 10 ml, for 15 min at room temperature, followed by centrifugation, and a second round of lysis with 3 ml, for 15 min at room temperature, followed by neutralization with 12 ml of iPS cell medium. Cells were pelleted and counted, recovering ~10^6 cells per mouse. Cells were resuspended, plated on feeders and cultured in iPS cell medium.

Immunofluorescence. Cells previously seeded in cover slips were fixed in 4% paraformaldehyde for 20 min, permeabilized (PBS 0.1% Triton X-100) for 15 min and blocked in FBS, for 1 h at room temperature. For the detection of OCT4 we used two antibodies with similar results, BD 611203, dilution 1:200, and Santa Cruz sc-5279, dilution 1:400; for NANOG, Novus NB100 58842, dilution 1:50; and for CDX2, Epitomics #2475-1, dilution 1:400. Cells were inspected under a Leica SP5 microscope equipped with white light laser and hybrid detection.

Chimera generation and germline contribution. For chimaera generation, *in vivo* iPS cells (5–7 cells per embryo, ~10 passages) were microinjected into C57BL/6J-*Tyr*$^{c\text{-}2J}$/J blastocysts and transferred to Crl:CD1 (ICR) pseudopregnant females. To study the contribution to germline, GFP-infected *in vivo* iPS cells (~14 passages) were similarly microinjected into blastocysts and the gonads from chimaeric male E14.5 embryos were isolated, fixed in 4% paraformaldehyde, and analysed for GFP fluorescence in whole mount with laser scanning confocal microscope SP5 from Leica, equipped with white light laser and hybrid detection. Lens used for imaging were ×20 (dry lens) 0.7 numerical aperture and ×63 (water lens) with a 1.2 numerical aperture.

RNA-seq methods. Total RNA was extracted from ES cells (JM8.F6 (ref. 20), Bruce4 (ref. 21), and CNIO in-house made C57BL6.10), *in vitro* iPS cells (3 from i4F-A MEFs and 2 from i4F-B MEFs) and *in vivo* iPS cells (3 from i4F-A mice and 3 from i4F-B mice), all with ~10 passages. 1 μg of total RNA, with RIN (RNA integrity number) numbers in the range 9.8 to 10 (Agilent 2100 Bioanalyzer), was used. PolyA+ fractions were processed using TruSeq Stranded mRNA Sample Preparation Kit (Agilent). The resulting directional cDNA libraries were sequenced for 40 bases in a single-read format (Genome Analyzer IIx, Illumina). The complete set of reads have been deposited in the GEO repository (accession number GSE48364). Reads were aligned to the mouse genome (GRCm38/mm10) with TopHat-2.0.4 (ref. 40) (using Bowtie 0.12.7 (ref. 41) and Samtools 0.1.16 (ref. 42), allowing two mismatches and five multihits. Transcripts assembly, estimation of their abundances and differential expression were calculated with Cufflinks 1.3.0 (ref. 40), using the mouse genome annotation data set GRCm38/mm10 from the UCSC Genome Browser.

Trophectoderm stem cell differentiation. ES and iPS cells (all with ~10 passages) were plated on feeders (7×10^4 cells per well in 6-well plates) in iPS cells medium and 24 h later medium was changed into TS differentiation medium that contained the following components: 3 volumes of RPMI 1640 (with 20% FBS, 1 mM pyruvate, 2 mM L-glutamine, 100 μM β-mercaptoethanol), 7 volumes of conditioned medium from mitomycin-C-inactivated fibroblasts, 25 pg ml^{-1} of FGF4 (R&D Systems, 235-F4-025) and 1 μg ml^{-1} of heparin (Sigma, H3149). Medium was changed every other day, and all cells were split once at day 2. For giant cell differentiation, trophoblast stem cell differentiated *in vivo* iPS cells and established trophoblast stem cells were plated on gelatine and cultured in RPMI 1640 (with 20% FBS, 1 mM pyruvate, 2 mM L-glutamine, 100 μM β-mercaptoethanol) in the absence of heparin and FGF4 for 3 days.

Analysis of trophectoderm lineage contribution. GFP-labelled ES cells or *in vivo* iPS cells (5–7 cells, all with ~14 passages) were aggregated or microinjected into 8-cell stage embryos using standard techniques[43]. Morulas were incubated overnight and observed under the confocal microscope in KSOM (Chemical International) microdrops under mineral oil. In some cases Tg.CAG-Katushka embryos[29] were used as recipients. To study the contribution of GFP-*in vivo* iPS cells to the placenta, blastocysts were transferred to pseudopregnant females and embryos (E14.5) with their placentas were collected in PBS and observed directly under a fluorescence-equipped stereomicroscope or fixed for immunostaining.

Analysis of mRNA levels. Total RNA was extracted from cell or tissue samples with Trizol (Invitrogen), following provider's recommendations and retrotranscribed into cDNA following the manufacturer's protocol (Maxima First Strand cDNA systhesis Kit for RT–qPCR, Fermentas). Quantitative real time–PCR was performed using Syber Green Power PCR Master Mix (Applied Biosystems) in an ABI PRISM 7700 thermocycler (Applied Biosystem). For input normalization, we used the housekeeping genes *Actb* (β-actin) or *Gapdh*. The primers used were: *Actb* forward primer: 5′-GGCACCACACCTTCTACAATG-3′, *Actb* reverse primer: 5′-GTGGTGGT GAAGCTGTAGCC-3′; *Ccne* forward primer: 5′-GTGGCTCCGACCTTTCAG TC-3′, *Ccne* reverse primer 5′-CACAGTCTTGTCAATCTTGGCA-3′; *Cdx2* forward primer 5′-CAAGGACGTGAGCATGTATCC-3′, *Cdx2* reverse primer 5′-GTAACCACCGTAGTCCGGGTA-3′; *E2A-c-Myc* forward primer, 5′-GGCTG GAGATGTTGAGAGCAA-3′, *E2A-c-Myc* reverse primer 5′-AAAGGAAATCC AGTGGCGC-3′; *Eomes* forward primer 5′-TTCACCTTCTCAGAGACACAGT TCAT-3′, *Eomes* reverse primer 5′-GAGTTAACCTGTCATTTTCTGAAGCC-3′; *Epcam* forward primer 5′-GCGGCTCAGAGAGACTGTG-3′, *Epcam* reverse primer 5′-CCAAGCATTTAGACGCCAGTTT-3′; *Etv4* forward primer, 5′-TGGTGAT CAAACAGGAGCG-3′, *Etv4* reverse primer, 5′-GGGTGGAGGTACATTGA TGC-3′; *Fgfr2* forward primer, 5′-GAGGAATACTTGGATCTCACC-3′, *Fgfr2* reverse primer 5′-CTGGTGCTGTCCTGTTTGGG-3′; *Gapdh* forward primer

5′-TTCACCACCATGGAGAAGGC-3′, *Gapdh* reverse primer 5′-CCCTTTTGG CTCCACCCT-3′; *Gata6* forward primer 5′-TCATTACCTGTGCAATGCATGC GG-3′, *Gata6* reverse primer 5′-ACGCCATAAGGTAGTGGTTGTGGT-3′; *Gbx2* forward primer 5′-CAACTTCGACAAAGCCGAGG-3′, *Gbx2* reverse primer 5′-ACTCGTCTTTCCCTTGCCCT-3′; *IAP* forward primer 5′-CAGACTGGGA GGAAGAAGCA-3′, *IAP* reverse primer 5′-ATTGTTCCCTCACTGGCAAA-3′; *Lin28a* forward primer 5′-GAAGAACATGCAGAAGCGAAGA-3′, *Lin28a* reverse primer 5′-CCGCAGTTGTAGCACCTGTCT-3′; *Mmp12* forward primer 5′-CT GCTCCCATGAATGACAGTG-3′, *Mmp12* reverse primer 5′-AGTTGCTTCTA GCCCAAAGAAC-3′; *MuERV-L* forward primer 5′-CCCATCATGAGCTGGGT ACT-3′, *MuERV-L* reverse primer 5′-CGTGCAGAGCCATCAGTAAA-3′; *Nanog* forward primer 5′-CAAGGGTCTGCTACTGAGATGCTCTG-3′, *Nanog* reverse primer 5′-TTTTGTTTGGGACTGGTAGAAGAATCAG-3′; *Neto2* forward primer 5′-GTCGTGGAAGGGATTGCTGT-3′, *Neto2* reverse primer 5′-AAGCA AAATGACCTCCATTGC-3′; *Nlrp4* forward primer 5′-TGTCCTGAATGAAG GAGACCA-3′, *Nlrp4* reverse primer 5′-TTACTCCTTACAAACACAGAGCA CA-3′; *Oct4* (total) forward primer 5′-GTTGGAGAAGGTGGAACCAA-3′, *Oct4* (total) reverse primer 5′-CCAAGGTGATCCTCTTCTGC-3′; *Pparg* forward primer 5′-GGCCGAGAAGGAGAAGCTGTTG-3′, *Pparg* reverse primer 5′-TGG CCACCTCTTTGCTCTGCTC-3′; *Ppm1j* forward primer 5′-AGAGCAGGCAC AATGAGGAT-3′, *Ppm1j* reverse primer 5′-CATCAAACAGGCCCCAGTAG-3′; *Sox1* forward primer, 5′-TGAACGCCTTCATGGTGTGGTC-3′, *Sox1* reverse primer 5′-GCGCGGCCGGTACTTGTAAT-3′; *Sox2* forward primer 5′-CGTA AGATGGCCCAGGAGAA-3′, *Sox2* reverse primer 5′-GCTTCTCGGTCTCGG ACAAA-3′; *Sox2-Klf4* forward primer 5′-ACTGCCCCTGTCGCACAT-3′, *Sox2-Klf4* reverse primer 5′-CATGTCAGACTCGCCAGGTG-3′; *T* forward primer 5′-GCTTCAAGGAGCTAACTAACGAG-3′, *T* reverse primer 5′-CCAGCAAGAA AGAGTACATGGC-3′; *Tgm1* forward primer 5′-CAGATCTGCCCTCAGGC TT-3′, *Tgm1* reverse primer 5′-CCATTCTTGACGGACTCCAC-3′; *Tnc* forward primer 5′-ACCATGGGTACAGGCTGTTG-3′, *Tnc* reverse primer 5′-CCTT CTGCACTGAAGTTGCC-3′; *Utf1* forward primer 5′-TGTCCCGGTGACTAC GTCT-3′, *Utf1* reverse primer 5′-CCCAGAAGTAGCTCCGTCTCT-3′; *Zscan4* forward primer 5′-GAGATTCATGGAGAGTCTGACTGATGAGTG-3′, *Zscan4* reverse primer 5′-GCTGTTGTTTCAAAAGCTTGATGACTTC-3′; *8430410A17Rik* forward primer 5′-TGGATTCTACGAGTGGCAGC-3′, *8430410A17Rik* reverse primer 5′-CTGTCTGAAGCATCGTTCCC-3′.

Protein analysis. Tissue samples (50–100 mg) were homogenized in medium-salt lysis buffer (150 mM NaCl, 50 mM Tris pH 8, 1% NP40 and protein inhibitors cocktail) using Precellys 24 homogenizer. A total protein amount of 30 μg was loaded per lane in a NuPAGE 4–12% Bis-Tris gel 1.0 mm (Invitrogen) and electrophoresed in MES SDS Running Buffer (Invitrogen). The following antibodies were used: for OCT4, Santa Cruz Biotechnology sc-9081, 1:500; for NANOG, Millipore AB 5731, 1:5,000; for SOX2, Santa Cruz sc-17320, 1:500; and for actin, Sigma-Aldrich AC-15, 1:5,000.

Immunohistochemistry. Tissue samples were fixed in 10% formaline, paraffine-embedded and cut in 3-μm sections, which were mounted in superfrostplus porta-objects and re-hydrated. For immunohistochemistry, paraffine sections underwent antigenic exposure process into the Discovery XT (Roche) system with CC1 buffer for standard antigen retrieval. The following primary antibodies were used: for NANOG, Cell Signalling Biotechnology, 8822; for cytokeratin 19 (CK19), CNIO Monoclonal Antibodies Core Unit, AM-TROMA III; for placental lactogen 1 (PL-1), Santa Cruz Biotechnology, sc34713; for cytokeratin 8 (CK8), CNIO Monoclonal Antibodies Core Unit, AM-TROMA I; for GFP, Roche, 11814460001; for SOX2, Cell Signaling Technology, 3728; for T/BRACHYURY, Santa Cruz Biotechnology, sc17743; for GATA4, Santa Cruz Biotechnology, sc1237; for CDX2, Biogenex, MU392A-UC; for α-fetoprotein (AFP), R&D Systems, AF5369; and for OCT4, Santa Cruz Biotechnology, sc-9081. Slides were then incubated with the corresponding secondary antibodies conjugated with peroxidase from Dako.

Statistical methods. Sample sizes for comparisons between cell types or between mouse genotypes followed Mead's recommendations[44]. In particular, the accumulated *n* value (*N*) for a given comparison minus the number of groups or treatments (T) (for example, genotypes) was between 10 and 20, as recommended[44]. Samples (cells or mice) were allocated to their experimental groups according to their pre-determined type (cell type or mouse genotype) and therefore there was no randomization. Investigators were not blinded to the experimental groups (cell types or mouse genotypes). In the case of Fig. 1e, no mice were censored. In the case of Fig. 2a, b, only mice that died with teratomas were considered, as indicated in the ordinate axes; mice that died due to other complications were censored and indicated with ticks in the Kaplan–Meier curves. Quantitative PCR data were obtained from independent biological replicates (*n* values indicated in the corresponding figure legends) and were tested for normal distribution using the Shapiro-Wilk test and for equal variance using the *F*-test. Normal distribution and equal variance was confirmed in the large majority of data and, therefore, we assumed normality and equal variance for all samples. Based on this, we used the Student's *t*-test (two-tailed, unpaired) to estimate statistical significance. For contingency tables, we used the Fisher's exact test.

39. Domínguez, O. & López-Larrea, C. Gene walking by unpredictably primed PCR. *Nucleic Acids Res.* **22,** 3247–3248 (1994).
40. Trapnell, C. *et al.* Differential gene and transcript expression analysis of RNA-seq experiments with TopHat and Cufflinks. *Nature Protocols* **7,** 562–578 (2012).
41. Langmead, B., Trapnell, C., Pop, M. & Salzberg, S. L. Ultrafast and memory-efficient alignment of short DNA sequences to the human genome. *Genome Biol.* **10,** R25 (2009).
42. Li, H. *et al.* The Sequence Alignment/Map format and SAMtools. *Bioinformatics* **25,** 2078–2079 (2009).
43. Pease, S. & Sounders, T. *Advanced Protocols for Animal Transgenesis, an ISTT Manual.* (Springer-Verlag, 2011).
44. Festing, M. F. W., Overend, P., Gaines Das, R., Cortina Borja, M. & Berdoy, M. *The design of animal experiments. Reducing the use of animals in research through better experimental design* (Royal Society of Medicine Press, 2002).

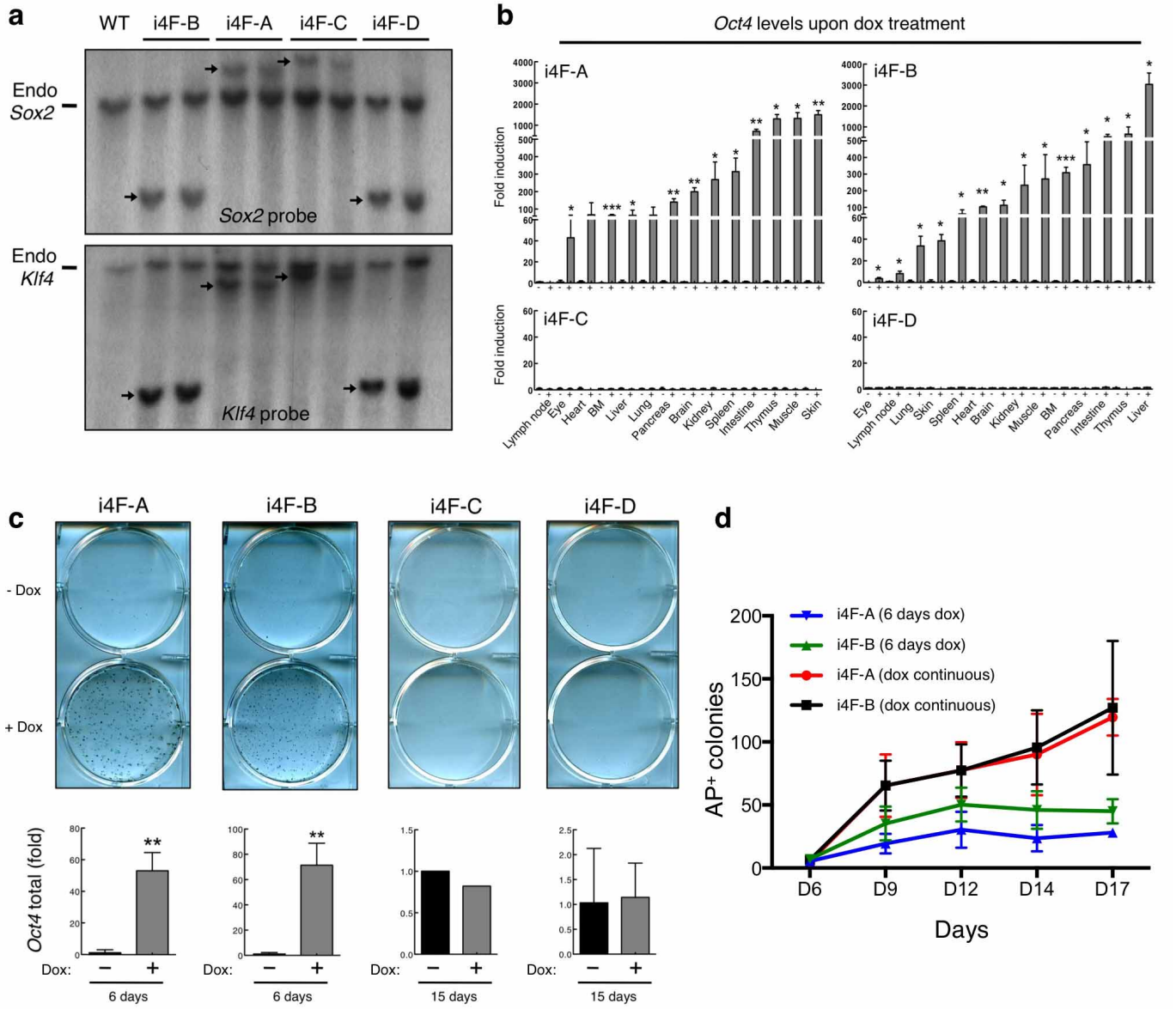

Extended Data Figure 1 | Characterization of four independent i4F transgenic mouse lines. **a**, Southern blot of tail tip genomic DNA digested with BamHI and hybridized with specific probes for *Sox2* and *Klf4*. **b**, Mice of the indicated transgenic lines carrying the reprogramming transgene (+) or without it (−) were treated with doxycycline (1 mg ml^{-1}) for 6 days. The mRNA levels of *Oct4* were determined by qRT–PCR. Values correspond to the average and s.d. ($n = 3$ mice per transgenic line) and are relative to the levels of wild-type mice treated with doxycycline. **c**, MEFs of the indicated mouse lines were treated with doxycyline (1 μg ml^{-1}). Colonies of iPS cells in the i4F-A and i4F-B plates were stained for alkaline phosphatase (AP) 10 days after induction. In the case of i4F-C and i4F-D, plates were stained after 15 days but no iPS cell colonies were observed. In parallel, total *Oct4* mRNA levels were measured at the indicated times by qRT–PCR. Values correspond to the average and s.d. For i4F-A, i4F-B, and i4F-D, $n = 3$ MEF preparations; for i4F-C, $n = 1$. **d**, Comparison of the *in vitro* reprogramming kinetics and efficiency of MEFs from lines i4F-A and i4F-B. Reprogramming was induced with two different protocols: 1 μg ml^{-1} of doxycycline for 6 days, or continuous treatment with 1 μg ml^{-1} of doxycycline. AP^{+} colonies were counted at the indicated times. Values correspond to the average and s.d. ($n = 3$ independent MEF isolates per line). In **b** and **c**, statistical significance was evaluated by the Student's *t*-test (unpaired, two-tailed): $*P < 0.05$, $**P < 0.01$, $***P < 0.001$.

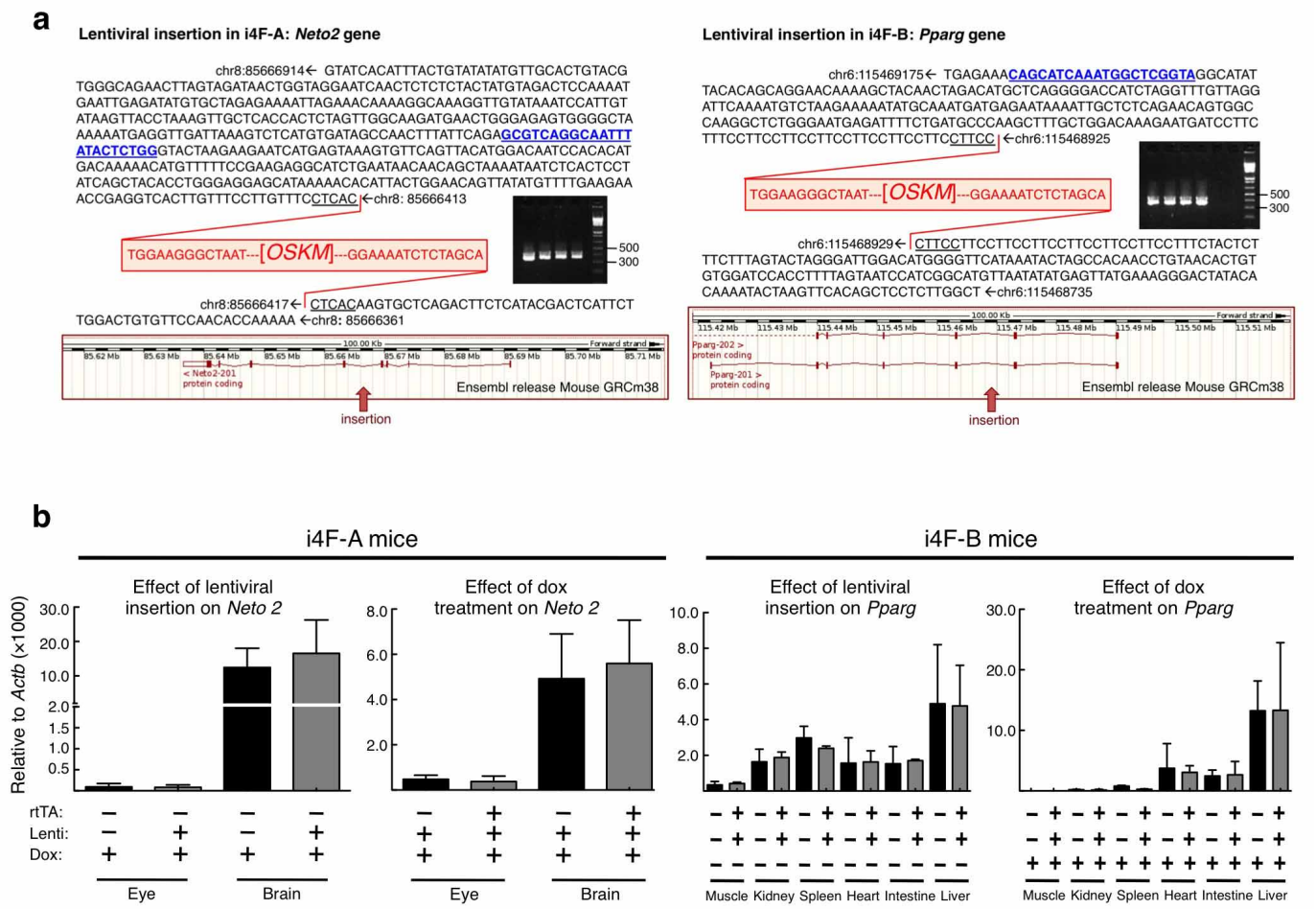

Extended Data Figure 2 | Genomic insertion sites of lentiviral transgenes i4F-A and i4F-B and their effect on the host genes. a, Primers used for PCR to confirm insertion are shown in blue and underlined. These primers were used together with a common primer hybridizing to internal lentiviral sequences (see Methods). The 4 base pairs flanking the insertion site are duplicated upon lentiviral insertion and are underlined. A map of each gene is shown indicating with an arrow the approximate location of the lentiviral transgene. The pictures of PCR agarose gels correspond to the PCR products obtained with the flanking primer (underlined sequence in blue) and the internal lentiviral primer (not shown) (see Methods). **b**, The indicated tissues were used to measure the levels of *Neto2* (host gene for the lentiviral transgene i4F-A) or *Pparg* (host gene for the lentiviral transgene i4F-B). Values correspond to the average and s.d. ($n = 3$ mice per condition). Statistical significance was evaluated by Student's *t*-test (unpaired, two-tailed). No significant differences were observed.

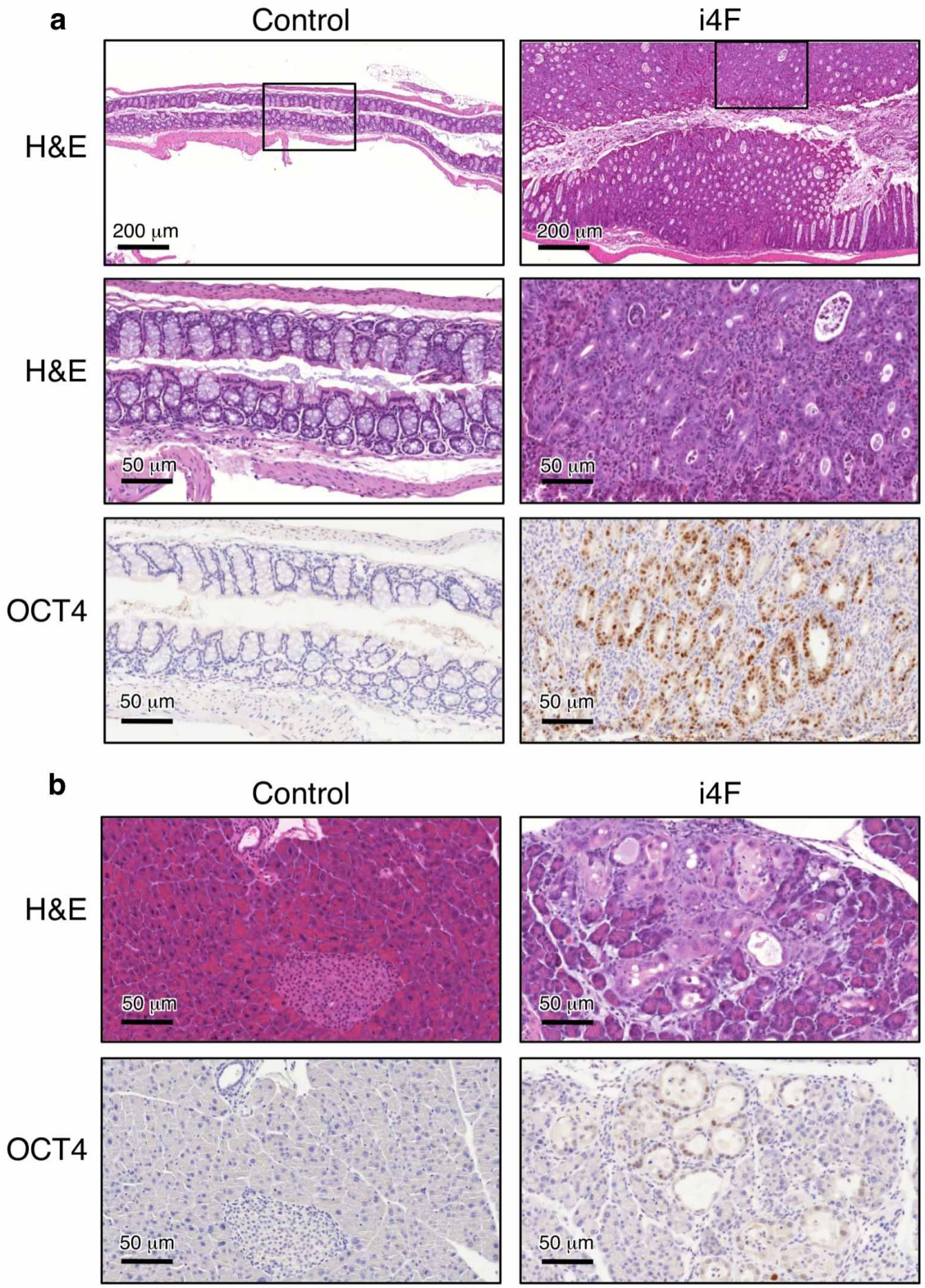

Extended Data Figure 3 | Histological alterations of the intestine and pancreas upon induction of i4F reprogrammable mice. Mice were treated with doxycycline (1 mg ml^{-1}) for 6 days. Haematoxylin and eosin (H&E) staining and inmunohistochemistry of OCT4 in the intestine (**a**) and pancreas (**b**). Similar alterations were found in both lines, i4F-A and i4F-B.

a

b

	Mice analyzed with teratomas	Teratomas	Other tumours in the same mice
i4F-A	8	Multiple per mouse	1 Wilm's tumour 1 skin papilloma 1 mouse with intestinal polyps
i4F-B	7	Multiple per mouse	1 urothelial carcinoma 1 mouse with intestinal polyps

c

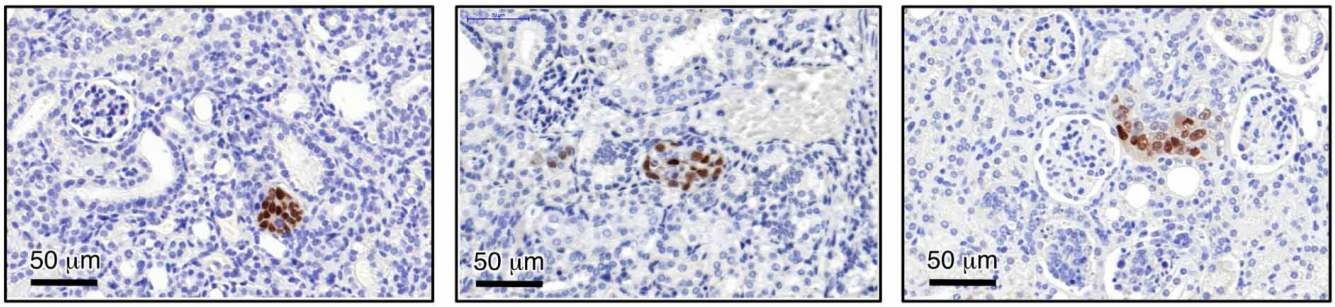

Extended Data Figure 4 | i4F induction leads to the appearance of tumoral masses and *in situ* reprogramming events. **a**, Reprogrammable mouse with multiple tumoral masses in the liver and kidneys (a representative example is shown from 15 mice analysed with teratomas). **b**, Incidence of other tumours in reprogrammable mice with teratomas. **c**, Three examples of NANOG-positive tubules in different induced reprogrammable mice.

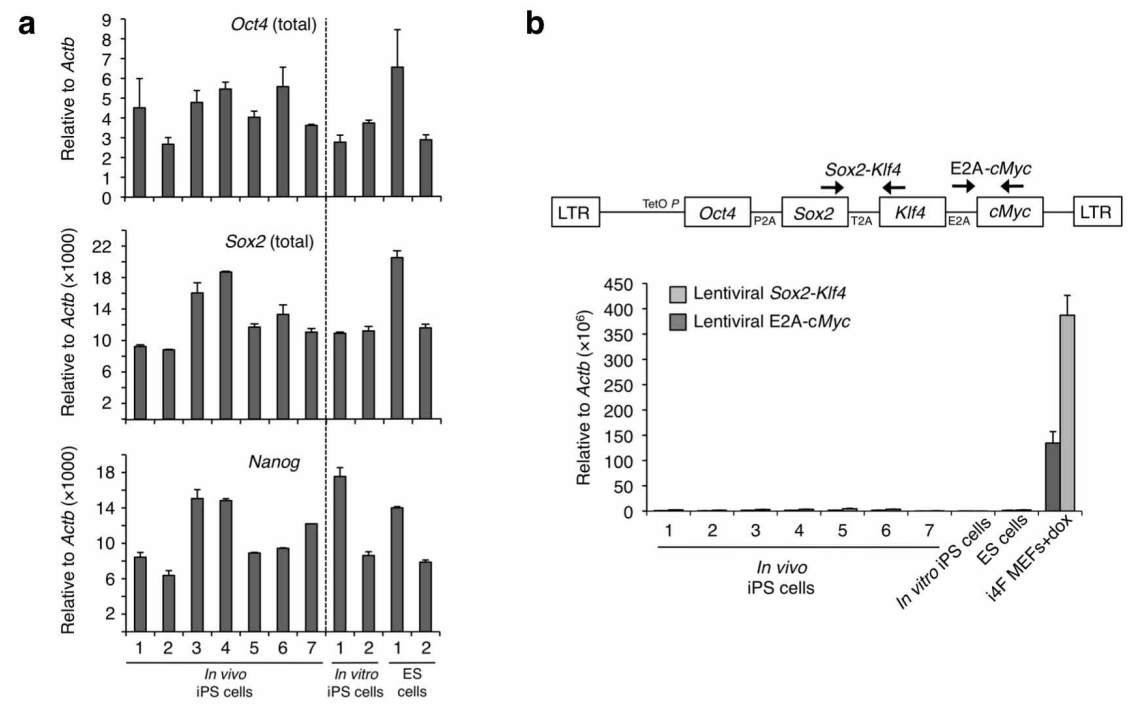

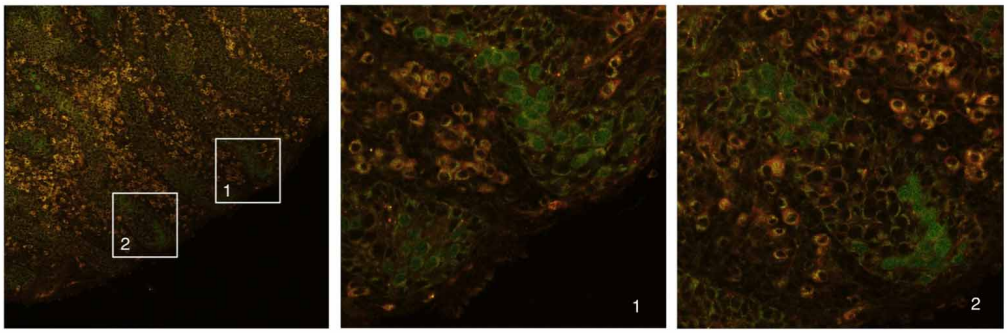

d

Reprogrammable mouse type	Strain	Dox (mg ml^{-1})	Mice analyzed	Mice with *in vivo* iPS cells in the blood
i4F whole body	i4F-A	0.2	5	0
	i4F-A	1.0	9	0
	i4F-B	0.2	13	2 (16 clones, 8 clones)
	i4F-B	1.0	8	0
i4F-BM in WT host	i4F-A	1.0	13	2 (1 clone, 10 clones)
	i4F-B	1.0	22	0
WT-BM in i4F host	i4F-B	0.2	7	1 (11 clones)
Total:			77	5 (9±5 clones) (6.5%)

Extended Data Figure 5 | Characterization of *in vivo* iPS cells. a, Expression of pluripotency markers in the indicated cell types. Data correspond to qRT–PCR from seven independent *in vivo* iPS cell clones, two *in vitro* iPS cell clones (no. 1: *in vitro* reprogrammed i4F MEFs; no. 2: *in vitro* reprogrammed wild-type MEFs infected with lenti-OSKM), and two ES cell clones (no. 1: C57BL6.10; no. 2: G4). Values correspond to the average ± s.d. of 3 technical replicates. **b**, Silencing of the lentiviral cassette in *in vivo* iPS cell clones. Upper part, location of the PCR primers used. Lower part, lentiviral RNA levels in *in vivo* iPS cells (7 independent clones), in an *in vitro* iPS cell clone (*in vitro* reprogrammed i4F MEFs), in an ES cell line (C57BL6.10), and in i4F-MEFs induced with doxycycline for 3 days. Values correspond to the average ± s.d. of 3 technical replicates. **c**, Chimaeric E14.5 testis generated with a GFP-labelled *in vivo* iPS cells. Magnifications show germ cells derived from *in vivo* iPS cells. **d**, Summary of the isolation of *in vivo* iPS cells from the bloodstream.

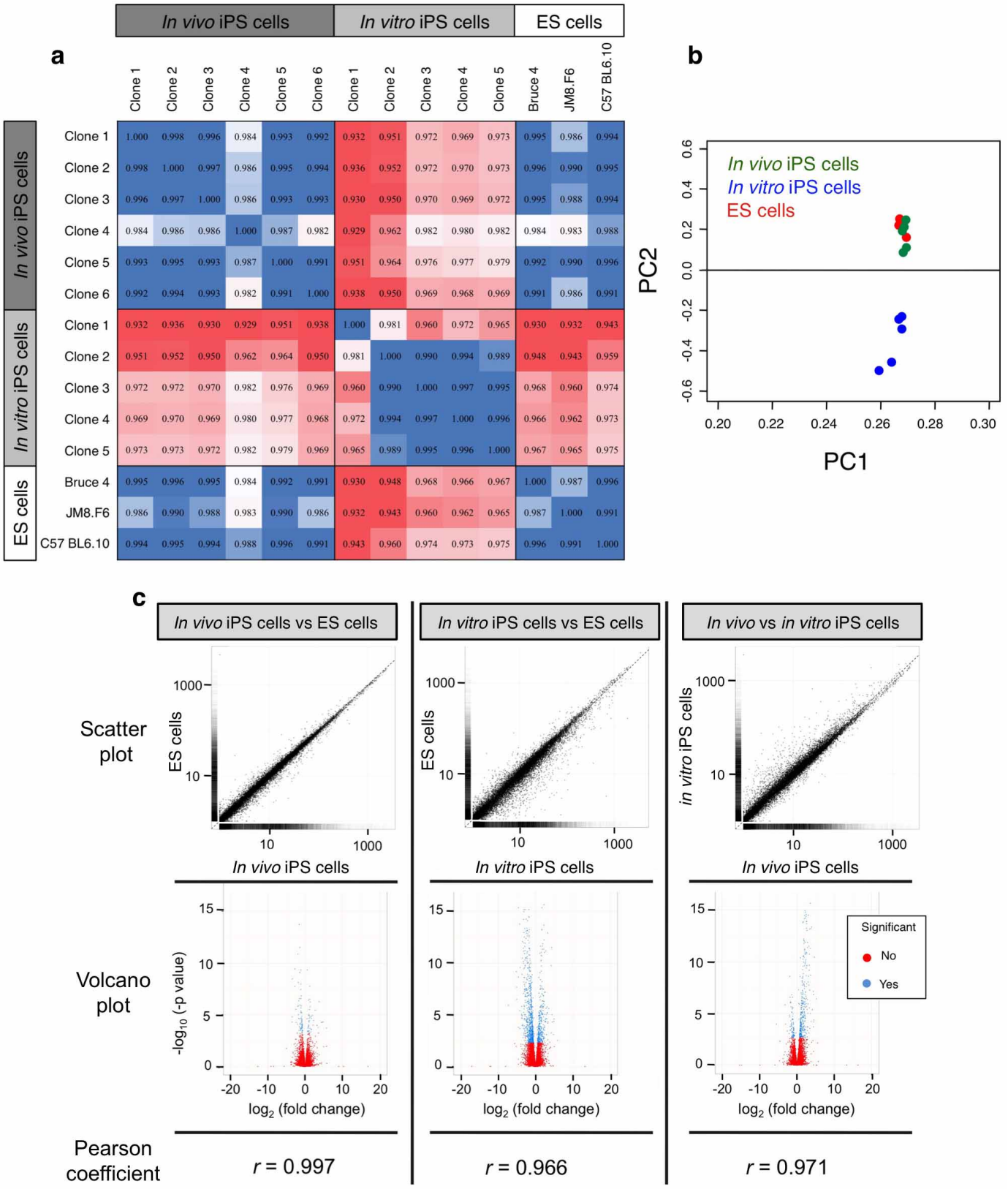

Extended Data Figure 6 | Transcriptomic profiles of *in vivo* iPS cells, *in vitro* iPS cells and ES cells. **a**, Pearson correlation coefficients among all sequenced samples. The highest and the lowest coefficients are coloured in a blue to red gradient. **b**, Principal component analysis of the transcriptomes of *in vivo* iPS cells, *in vitro* iPS cells and ES cells. Data correspond to 6 clones of *in vivo* iPS cells, 5 clones of *in vitro* iPS cells, and 3 lines of ES cells (C57BL6.10, JM8.F6 and Bruce4). **c**, Upper part, scatter plots representing the expression of each gene in the indicated pairs of cell types. Middle part, volcano plots representing the *P* value of the differences in expression of each gene between the corresponding cell types. Significant *P* values are in blue (that is, indicating differentially expressed genes). Non-significant *P* values are in red (that is, indicating genes that are not differentially expressed). Lower part, Pearson coefficient correlation among samples. Data correspond to 6 clones of *in vivo* iPS cells, 5 clones of *in vitro* iPS cells, and 3 lines of ES cells (C57BL6.10, JM8.F6 and Bruce4).

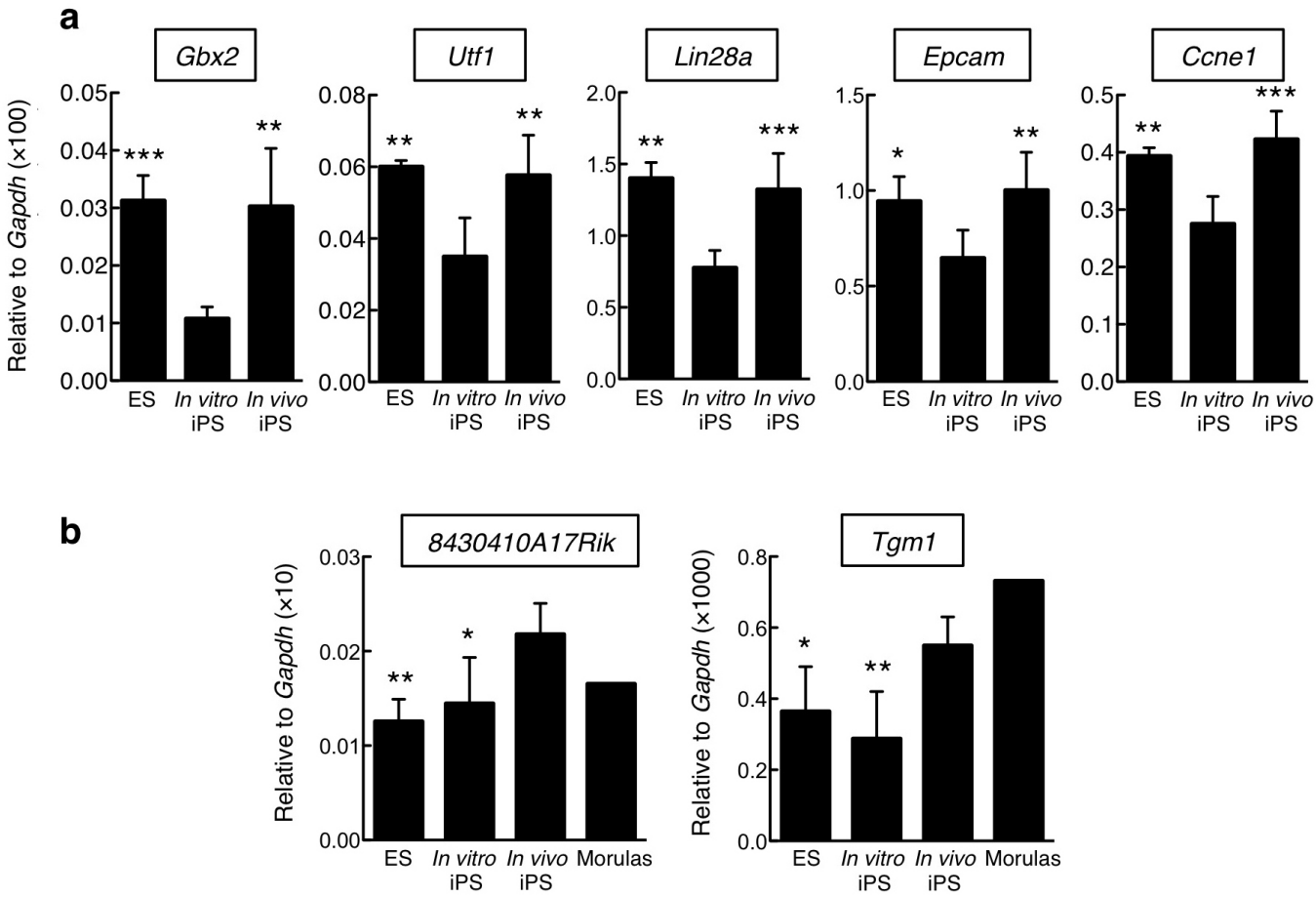

Extended Data Figure 7 | Validation of RNA-seq data. **a**, Genes upregulated in *in vivo* iPS and ES cells versus *in vitro* iPS cells. **b**, Genes upregulated in *in vivo* iPS cells versus ES cells and *in vitro* iPS cells. Expression levels of the indicated genes in *in vivo* iPS cells ($n = 6$ clones), *in vitro* iPS cells ($n = 5$ clones) and ES cells ($n = 3$ lines C57BL6.10, JM8.F6 and Bruce4). A sample of RNA derived from a preparation of ~170 morulas was also included in **b**. Values correspond to the average ± s.d. Statistical significance was evaluated relative to *in vitro* iPS cells (**a**) or relative to *in vivo* iPS cells (**b**) by the Student's *t*-test (unpaired, two-tailed): $*P < 0.05$, $**P < 0.01$, $***P < 0.001$.

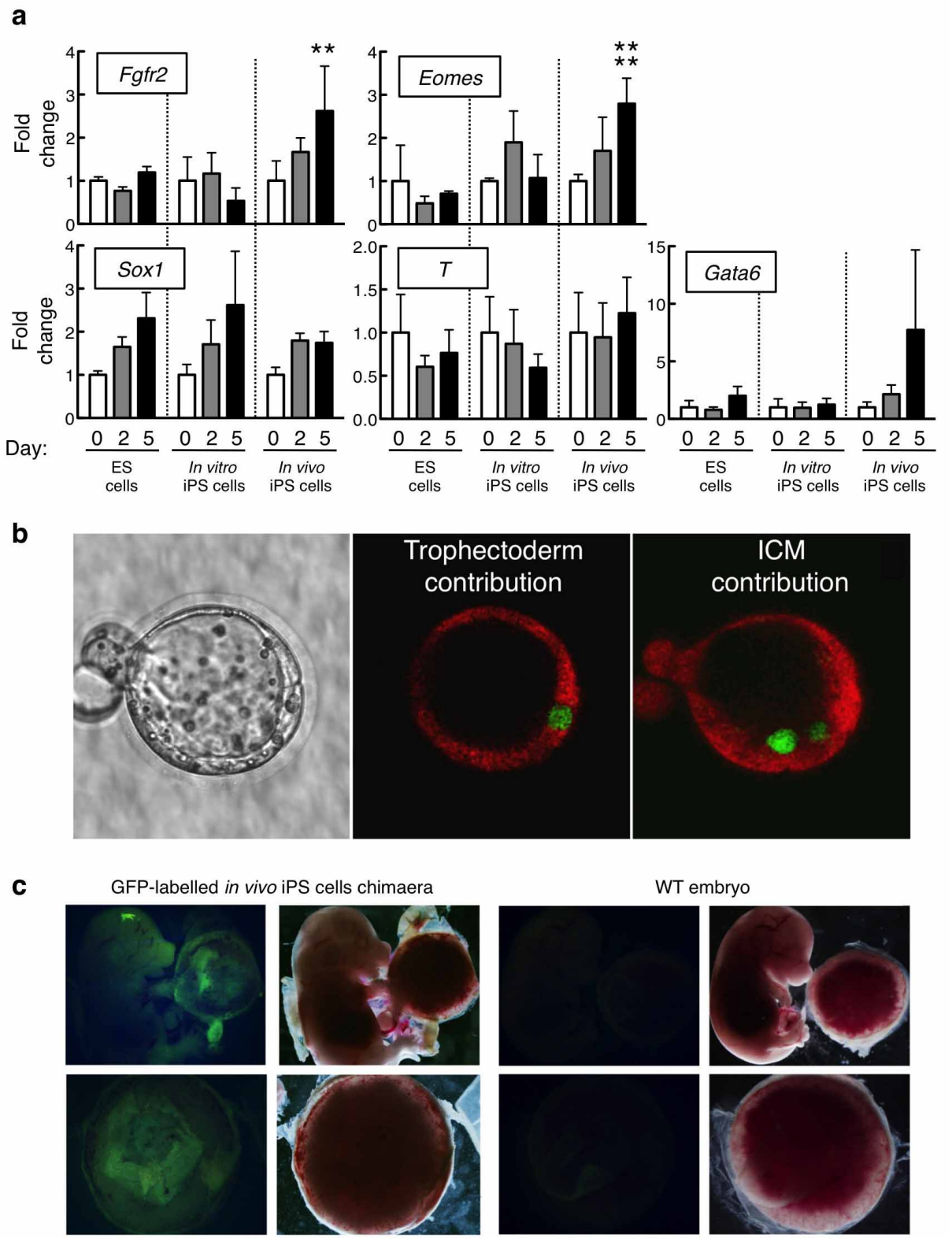

Extended Data Figure 8 | *In vivo* iPS cell contribution to the trophectoderm lineage. **a**, Induction of trophectoderm markers (*Fgfr2, Eomes*) in the indicated cell types after culture in TS differentiation medium (see Methods) during the indicated period of time. Other markers were used as controls: *Sox1* (ectoderm), *T* (mesoderm) and *Gata6* (endoderm). For each cell type, values are relative to the average levels at day 0. Values correspond to the average and s.d. For ES cells, $n = 3$ (lines C57BL6.10, JM8.F6 and Bruce4); for *in vitro* iPS cells, $n = 5$ clones; and for *in vivo* iPS cells, $n = 5$ clones. Statistical significance was determined using the Student's *t*-test (unpaired, two-tailed): $^{*}P < 0.05$, $^{**}P < 0.01$. The lower line of asterisks refers to the comparison with *in vitro* iPS cells, and the upper line of asterisks to the comparison with ES cells. **b**, Example of a chimaeric blastocyst derived from a Katushka morula injected with GFP-labelled *in vivo* iPS cells. Two different confocal planes are shown containing GFP-labelled cells that have contributed to the trophectoderm and to the inner cell mass, as indicated. **c**, Chimaerism of GFP-labelled *in vivo* iPS cells in the proper embryo and placenta (E14.5). A wild-type embryo at the same stage of development is shown as a control. Fluorescence pictures were taken with the same settings.

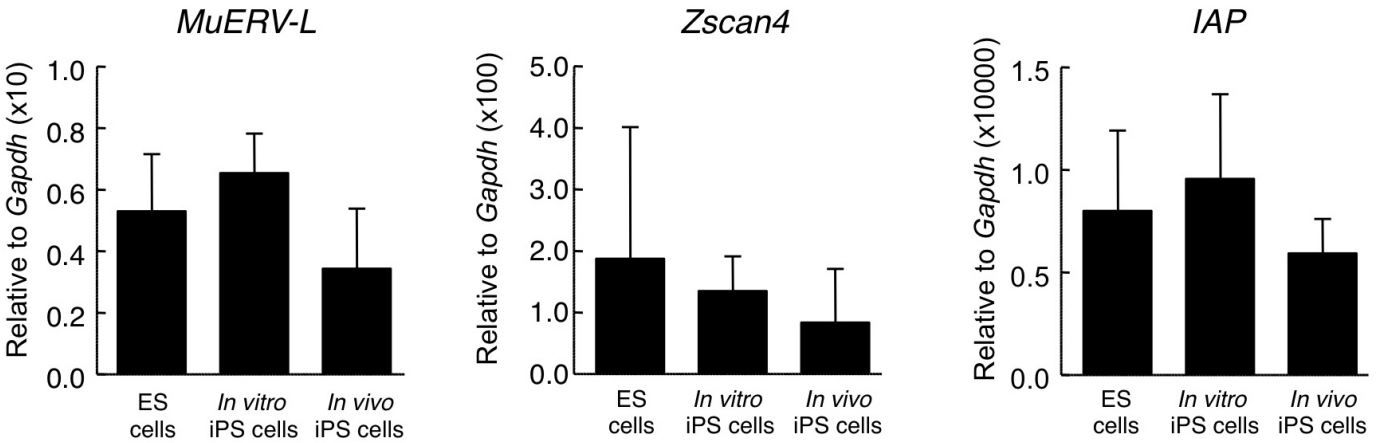

Extended Data Figure 9 | Expression levels of 2C marker genes. Analysis of the expression of genes enriched in the 2C state: the retrotrasposable elements *MuERV-L*, *Zscan4*, and intracisternal A particles (*IAP*) showed no differences between *in vivo* iPS cells compared to ES cells and *in vitro* iPS cells. For ES cells, $n = 3$ (lines C57BL6.10, JM8.F6 and Bruce4); for *in vitro* iPS cells, $n = 5$ clones; and for *in vivo* iPS cells, $n = 6$ clones. Values correspond to the average and s.d. Statistical significance was determined using the Student's *t*-test (unpaired, two-tailed). None of the differences was statistically significant.

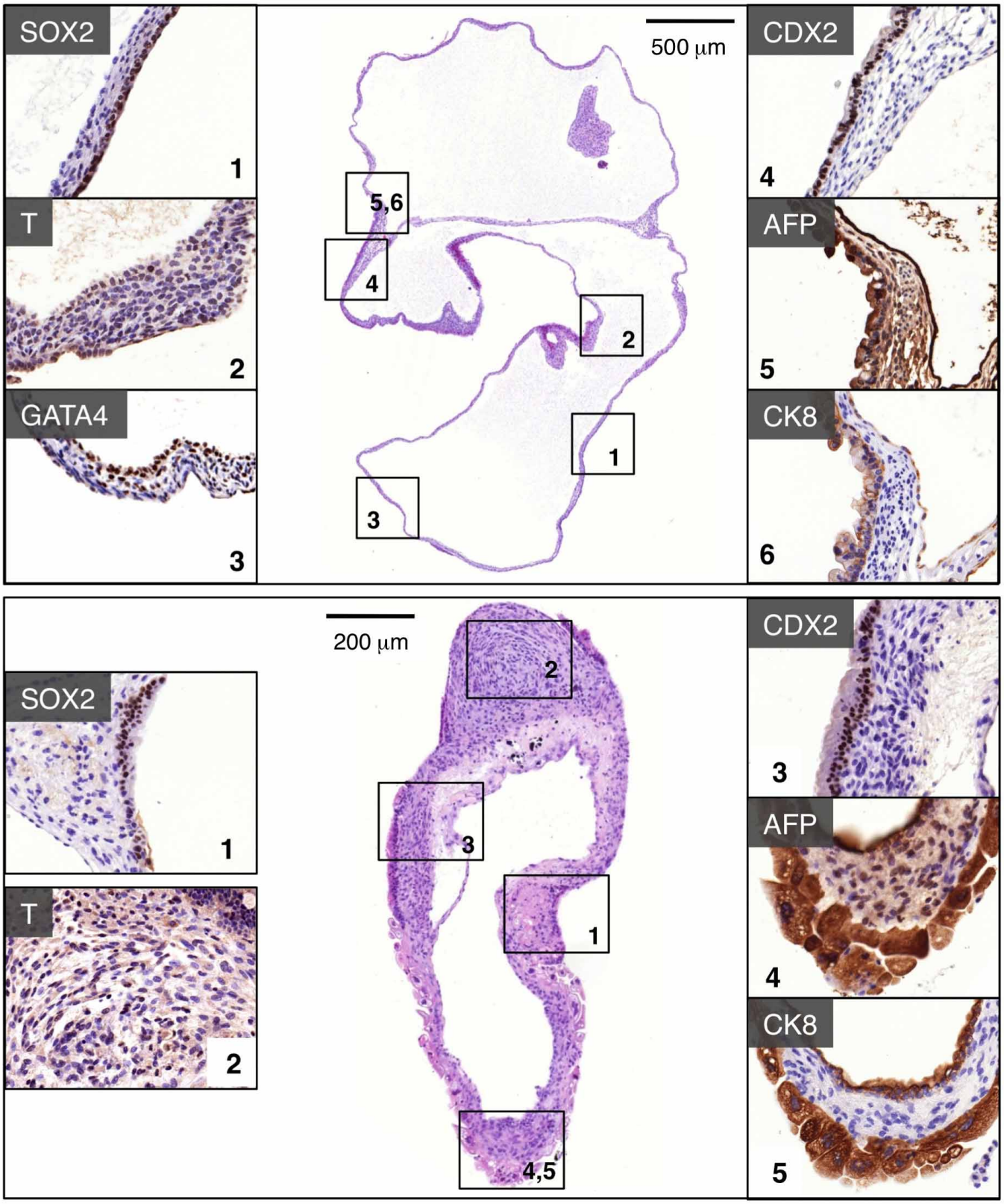

Extended Data Figure 10 | Immunohistochemical characterization of embryo-like structures. Haematoxylin and eosin and immunostaining analysis of two examples of embryo-like structures generated upon *in vivo* iPS cells intraperitoneal injection. The following markers were used: SOX2 (ectoderm), T/BRACHYURY (mesoderm), GATA4 (endoderm), CDX2 (trophectoderm), AFP and CK8 (visceral endoderm of the yolk sac). All lateral panels are at the same magnification.